Angular distribution of the FCNC process $B_c \to D_s^*(\to D_s\pi)\ell^+\ell^-$

Yu-Shuai Li[1,2,3,5,†] and Xiang Liu[1,2,3,4,5,*]

[1]*School of Physical Science and Technology, Lanzhou University, Lanzhou 730000, China*
[2]*Lanzhou Center for Theoretical Physics, Key Laboratory of Theoretical Physics of Gansu Province, Lanzhou University, Lanzhou 730000, China*
[3]*Key Laboratory of Quantum Theory and Applications of MoE, Lanzhou University, Lanzhou 730000, China*
[4]*MoE Frontiers Science Center for Rare Isotopes, Lanzhou University, Lanzhou 730000, China*
[5]*Research Center for Hadron and CSR Physics, Lanzhou University and Institute of Modern Physics of CAS, Lanzhou 730000, China*

(Received 18 September 2023; accepted 27 October 2023; published 20 November 2023)

In this work, we study the flavor-changing neutral-current process $B_c \to D_s^*(\to D_s\pi)\ell^+\ell^-$ ($\ell = e, \mu, \tau$). The relevant weak transition form factors are obtained by using the covariant light-front quark model, in which the main inputs, i.e., the meson wave functions of B_c and D_s^*, are adopted as the numerical wave functions from the solution of the Schrödinger equation with the modified Godfrey-Isgur model. With the obtained form factors, we further investigate the relevant branching fractions and their ratios, and some angular observables, i.e., the forward-backward asymmetry $A_{\rm FB}$, the polarization fractions $F_{L(T)}$, and the CP-averaged angular coefficients S_i and the CP asymmetry coefficients A_i. We also present our results of the clean angular observables $P_{1,2,3}$ and $P'_{4,5,6,8}$, which can reduce the uncertainties from the form factors. Our results show that the corresponding branching fractions of the electron or muon channels can reach up to 10^{-8}. With more data being accumulated in the LHCb experiment, our results are helpful for exploring this process, and deepen our understanding of the physics around the $b \to s\ell^+\ell^-$ process.

DOI: 10.1103/PhysRevD.108.093005

I. INTRODUCTION

The flavor-changing neutral-current (FCNC) process, like the $b \to s\ell^+\ell^-$ ($\ell = e, \mu, \tau$) we are concerned with has attracted the attention of both theorists and experimentalists, and of course has been widely studied. The FCNC process is forbidden at the tree level, and can only operate through loop diagrams in the Standard Model (SM). At the lowest order, three amplitudes contribute to the decay width, i.e., the photo penguin diagram, the Z penguin diagram, and the W^+W^- box diagram. In all three diagrams, the virtual t quark plays a dominant role, while the c and u quarks are the secondary contributions. The FCNC process is very sensitive to the new physical effects. This suggests that it can serve as a perfect platform to search directly for new physics (NP) beyond the SM [1–3].

The $b \to s\ell^+\ell^-$ in the bottom(-stranged) mesons sector is an attractive experimental topic. The experimental search of the FCNC processes $B \to K^{(*)}\ell^+\ell^-$ started in 1998 [4–6]. The first observation of $B \to K\ell^+\ell^-$ was made by the Belle collaboration in 2001 with a statistical significance of 5.3 [7]. From 2001 to now, the $B \to K^{(*)}\ell^+\ell^-$ with $\ell^+\ell^-$ being either an e^+e^- or $\mu^+\mu^-$ pair has been observed or measured by the Belle [7–12], the *BABAR* [13–15], the CDF [16], the CMS [17], and the LHCb collaborations [18–23]. In particular, the LHCb collaboration measured the form-factor-independent observable P'_5 [23], and found a 2.5 standard deviation (σ) discrepancy to the SM prediction [24] after integrating over $1.0 < q^2 < 6.0\ \text{GeV}^2$. In addition, the LHCb collaboration recently reported the most precise measurement of the ratio of branching fractions for $B^+ \to K^+\mu^+\mu^-$ and $B^+ \to K^+e^+e^-$ decays in $1.1 < q^2 < 6.0\ \text{GeV}^2$ as $R_K^{\mu e} = 0.846^{+0.044}_{-0.041}$ [22], indicating a 3.1σ discrepancy with the SM prediction [2,25], and providing evidence for the violation of lepton flavor universality (LFU). For the B_s decays, there have been some experiments, such as the CDF [26,27] and the DØ experiments [28], to search for the $B_s \to \phi\ell^+\ell^-$ mode. In 2011, the $B_s \to \phi\mu^+\mu^-$ mode was first observed in the CDF experiment [29], and then measured by the CDF [16] and the LHCb collaborations [30–32]. The electron mode is still missing in the experiment. Moreover, in Ref. [32] the LHCb collaboration also

[†]Corresponding author: xiangliu@lzu.edu.cn
[†]liysh20@lzu.edu.cn

reported their measurement of the $B_s \to f_2'(1525)\mu^+\mu^-$ process. Compared to the dielectronic and dimuonic modes, the ditauic mode is less studied. There is a Belle experiment, which focused on the $B^0 \to K^{*0}\tau^+\tau^-$ process, and determined the upper limit of the branching fraction $\mathcal{B}(B^0 \to K^{*0}\tau^+\tau^-) < 3.1 \times 10^{-3}$ at 90% confidence level [33].

The FCNC decay of bottom(-stranged) mesons has also been studied by various theoretical approaches, such as the lattice QCD (LQCD) [34–36], the light-cone sum rule [37–49], the QCD factorization [50], the perturbative QCD (pQCD) [51–56] and its combination with LQCD data [57,58], as well as various quark models [59–65], and so on [66–68]. On the other hand, in order to understand the discrepancy of the value of R with the SM prediction, the effects beyond the SM are considered. Following this line of thought, the extensions of the SM via the extended Higgs-boson [69–75], supersymmetry [76,77], and extra dimensions [78] have been used. At the same time, some NP models with an additional heavy neutral boson [79–91] or leptoquarks [92–108] were also considered.

Although great progress has been made both experimentally and theoretically in the rare semileptonic decays of bottom(-strange) mesons in recent decades, those of bottom-charmed mesons have been less studied. Compared to the $B_{(s)}$ mesons, the B_c meson is difficult to produce at the Belle experiment because the $B_c\bar{B}_c$ is close to 12.5 GeV, which is far from the energy region of $\Upsilon(4S)$. Moreover, according to $f_c/f_u = (7.5 \pm 1.8) \times 10^{-3}$ measured by the LHCb collaboration [109], the B_c meson is also underproductivity in the pp experiment. Here, the f_c and f_u are the fragmentation fractions of B_c and B meson, respectively, in pp collisions. As a result, the B_c meson decay has received less experimental attention in the past. Recently, the LHCb collaboration reported the result of the $B_c^+ \to D_s^+\mu^+\mu^-$ process [110]. Using the pp collision data collected by the LHCb experiment at the center-of-mass energies of 7, 8, and 13 TeV, corresponding to a total integrated luminosity of 9 fb^{-1}, the LHCb collaboration did not observe significant signals in the nonresonant $\mu^+\mu^-$ modes, but set an upper limit as $f_c/f_u \times \mathcal{B}(B_c^+ \to D_s^+\mu^+\mu^-) < 9.6 \times 10^{-8}$ at the 95% confidence level. Moreover, considering that the $B_c \to D_s^{(*)}\ell^+\ell^-$ channels have similar amounts of branching fractions [111], and the D_s^* needs to be reconstructed by the D_s meson in the experiment, the measurement of $B_c \to D_s^*\ell^+\ell^-$ will be more difficult. This indicates that the search for rare semileptonic decays of B_c is difficult for the present experiment. However, with the high-luminosity upgrade of the Large Hadron Collider (LHC), this situation is likely to improve. In any case, with the accumulation of data in the experiment, we expect the LHCb experiment to search for these rare semileptonic decays of the B_c meson.

In the theoretical sector, the rare semileptonic decays of B_c have been studied by the light-front quark model (LFQM) [112], the pQCD [111], the QCD sum rule [113,114], the constituent quark model (CQM) [112]. The branching fractions of $B_c \to D_s^*\ell^+\ell^-$ with $\ell = e$ or μ are predicted to be approximately 10^{-7}. In Refs. [115–117], the $B_c \to D_s^*\mu^+\mu^-$ process was been studied within the SM and beyond. In this work, we also focus on the $B_c \to D_s^*\ell^+\ell^-$ process, where the necessary form factors are calculated via the covariant LFQM approach. To provide more physical observables, we present the angular distribution of the quasi-four-body process $B_c \to D_s^*(\to D_s\pi)\ell^+\ell^-$.

The applications of the standard and(or) covariant LFQM have proved successful in the study of the meson [118–157] and baryon weak decays [158–185]. The $B_c \to D_s^*$ weak transition form factors deduced by (axial)-vector currents have been calculated in Ref. [154] with the covariant LFQM. Probably in the series of papers [124–134,137–140,144–153,155,158–181], the hadron wave function was taken as a Gaussian-like form with phenomenal parameter β, which represents the hadron structure. To fix the phenomenal parameter, the corresponding decay constant was used. However, as we all know, the decay constant is only associated with the zero-point wave function. This indicates that the oversimplified Gaussian-form wave function is not able to depict the behavior far away from the zero point. For this object, we propose to directly adopt the numerical spatial wave function by solving the Schrödinger equation with the modified Godfrey-Isgur (GI) model. By fitting the mass spectrum of the observed heavy flavor mesons, the parameters of the potential model can be fixed. This strategy avoids the β dependence, and can also reduce the corresponding uncertainty. We note that in Ref. [186], the authors used a relativistic quark model based on the quasipotential approach in QCD to study the semileptonic decay of bottom mesons. In their approach, the numerical wave functions of the mesons are obtained, thus avoiding the corresponding uncertainty.

This paper is organized as follows. After the Introduction, we illustrate the angular distributions of the quasi-four-body decays $B_c \to D_s^*(\to D_s\pi)\ell^+\ell^-$ ($\ell = e, \mu, \tau$) in Sec. II. In Sec. III, we introduce the covariant LFQM and derive the formula of the weak transition form factors. Then in Sec. IV, the numerical results, including the from factors of $B_c \to D_s^*$ and physical observables of $B_c \to D_s^*(\to D_s\pi)\ell^+\ell^-$ processes, are presented. Finally, this paper ends with a short summary.

II. THE ANGULAR DISTRIBUTION OF $B_c \to D_s^*(\to D_s\pi)\ell^+\ell^-$

A. The effective Hamiltonian for $b \to s\ell^+\ell^-$

The effective Hamiltonian associated with $b \to s\ell^+\ell^-$ is [187]

$$\mathcal{H} = -\frac{4G_F}{\sqrt{2}}\Big\{V_{tb}V_{ts}^*\Big[C_1(\mu)\mathcal{O}_1^c(\mu) + C_2(\mu)\mathcal{O}_2^c(\mu) + \sum_{i=3}^{10} C_i(\mu)\mathcal{O}_i(\mu)\Big] + V_{ub}V_{us}^*[C_1(\mu)(\mathcal{O}_1^c(\mu) - \mathcal{O}_1^u(\mu)) + C_2(\mu)(\mathcal{O}_2^c(\mu) - \mathcal{O}_2^u(\mu))]\Big\}, \quad (2.1)$$

where V_{ij} are the Cabibbo-Kobayashi-Maskawa (CKM) matrix elements and $G_F = 1.16637 \times 10^{-5}$ GeV^{-2} [188] is the Fermi constant. Also, the $C_i(\mu)$ are Wilson coefficients and the $\mathcal{O}_i(\mu)$ are four fermion operators. They all depend on the QCD renormalization scale μ. More specifically, the $\mathcal{O}_{1,2}^{c,u}$ are current-current operations, the $\mathcal{O}_{3-6}$ are QCD penguin operators, the $\mathcal{O}_{7,8}$ are electromagnetic and chromomagnetic penguin operators, and the $\mathcal{O}_{9,10}$ are semileptonic operators, respectively.

Apart from the γ and Z penguin diagrams, and the W^+W^- box diagram, the long distance contribution, via the intermediate vector states $(\rho, \omega, \phi.J/\psi, \psi(2S), \ldots)$ (see Fig. 1) also shows an unignorable influence. By adding the factorable quark-loop contributions from $\mathcal{O}_{1-6,8}$ to the effective Wilson coefficients $C_{7,9}^{\rm eff}$, the effective Hamiltonian in Eq. (2.1) can be simplified. In the calculation, we have adopted the following effective Hamiltonian, i.e.,

$$\mathcal{H}^{\rm eff}(b \to s\ell^+\ell^-) = -\frac{4G_F}{\sqrt{2}}V_{tb}V_{ts}^*\frac{\alpha_e}{4\pi}\Big\{\bar{s}[C_9^{\rm eff}(q^2,\mu)\gamma^\mu P_L - \frac{2m_b}{q^2}C_7^{\rm eff}(\mu)i\sigma^{\mu\nu}q_\nu P_R]b(\bar{\ell}\gamma_\mu\ell) + C_{10}(\mu)(\bar{s}\gamma^\mu P_L b)(\bar{\ell}\gamma_\mu\gamma_5\ell)\Big\}, \quad (2.2)$$

where $P_{L(R)} = (1 \mp \gamma_5)/2$, $\sigma^{\mu\nu} = i(\gamma^\mu\gamma^\nu - \gamma^\nu\gamma^\mu)/2$, and the electromagnetic coupling constant $\alpha_e = 1/137$. The $\mathcal{C}_7^{\rm eff}$ and $\mathcal{C}_9^{10}$ are the effective Wilson coefficients, defined as [189]

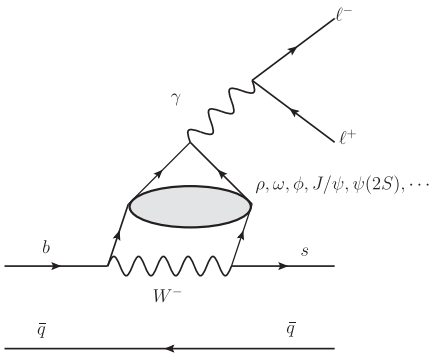

FIG. 1. The contributions of the intermediate vector states $(\rho, \omega, \phi.J/\psi, \psi(2S), \ldots)$ to the $b \to s\ell^+\ell^-$ process resulting from the current-current operators $\mathcal{O}_{1,2}^{c,u}$.

$$C_7^{\rm eff}(\mu) = C_7(\mu) + C'_{b\to s\gamma}(\mu),$$
$$C_9^{\rm eff}(q^2,\mu) = C_9(\mu) + Y_{\rm pert}(q^2,\mu) + Y_{\rm res}(q^2,\mu), \quad (2.3)$$

where the term $C'_{b\to s\gamma}$ is the absorptive part of the $b \to sc\bar{c} \to s\gamma$ rescattering [54,57,58,64,76,189–191]:

$$C'_{b\to s\gamma}(\mu) = i\alpha_s\Big\{\frac{2}{9}\eta^{\frac{14}{23}}\Big[\frac{x_t(x_t^2 - 5x_t - 2)}{8(x_t-1)^3} + \frac{3x_t^2\ln x_t}{4(x_t-1)^4} - 0.1687\Big] - 0.03C_2(\mu)\Big\} \quad (2.4)$$

with $x_t = m_t^2/m_W^2$, $\eta = \alpha_s(m_W)/\alpha_s(\mu)$, and α_s being adopted as $\alpha_s(m_b) = 0.217$ in our calculation. The short-distance contributions from the soft-gluon emission and the one-loop contributions of the four fermion operators $\mathcal{O}_1 - \mathcal{O}_6$, and the long-distance contributions from the intermediate vector meson states are also taken into account, and have been included in the $Y_{\rm pert}$ and $Y_{\rm res}$ terms, respectively. The $Y_{\rm pert}$ can be written as [192]

$$\begin{aligned} Y_{\rm pert}(\hat{s},\mu) = {} & 0.124\omega(\hat{s}) + g(\hat{m}_c,\hat{s})C(\mu) \\ & + \lambda_\mu\Big[g(\hat{m}_c,\hat{s}) - g(0,\hat{s})\Big](3C_1(\mu) + C_2(\mu)) \\ & - \frac{1}{2}g(0,\hat{s})(C_3(\mu) + 3C_4(\mu)) \\ & - \frac{1}{2}g(1,\hat{s})(4C_3(\mu) + 4C_4(\mu) + 3C_5(\mu) + C_6(\mu)) \\ & + \frac{2}{9}(3C_3(\mu) + C_4(\mu) + 3C_5(\mu) + C_6(\mu)), \end{aligned} \quad (2.5)$$

where $\hat{s} = q^2/m_b^2$ and $\hat{m}_c = m_c/m_b$ with $m_b = 4.8$ GeV and $m_c = 1.6$ GeV, and $C(\mu) = 3C_1(\mu) + C_2(\mu) + 3C_3(\mu) + C_4(\mu) + 3C_5(\mu) + C_6(\mu)$. At the next leading order, the Wilson coefficients at the QCD renormalization scale $\mu = m_b$ are chosen as $C_1 = -0.175$, $C_2 = 1.076$, $C_3 = 1.258\%$, $C_4 = -3.279\%$, $C_5 = 1.112\%$, $C_6 = -3.634\%$, $C_7 = -0.302$, $C_8 = -0.148$, $C_9 = 4.232$, and $C_{10} = -4.410$ [187].

In the Wolfenstein representation, the $\lambda_u = V_{ub}V_{us}^*/(V_{tb}V_{ts}^*)$ can be expressed as

$$\lambda_u \approx -\lambda^2(\rho - i\eta), \quad (2.6)$$

approximately, which is a small value suppressed by λ^2 with $\lambda = 0.22500 \pm 0.00067$ [188].

In addition, the term $\Omega(\hat{s})$ is the one-gluon correction to the matrix element of the operator $\mathcal{O}_9$, represented as [57,192]

$$\omega(\hat{s}) = -\frac{2}{9}\pi^2 + \frac{4}{3}\int_0^{\hat{s}} \frac{\ln 1-u}{u} du - \frac{2}{3}\ln(\hat{s})\ln(1-\hat{s}) - \frac{5+4\hat{s}}{3(1+2\hat{s})}\ln(1-\hat{s}) - \frac{2\hat{s}(1+\hat{s})(1-2\hat{s})}{3(1-\hat{s})^2(1+2\hat{s})}\ln(\hat{s}) + \frac{5+9\hat{s}-6\hat{s}^2}{6(1-\hat{s})(1+2\hat{s})}, \tag{2.7}$$

and the g terms [54,64,76,190,192]:

$$g(z,\hat{s}) = -\frac{8}{9}\ln z + \frac{8}{27} + \frac{4}{9}x - \frac{2}{9}(2+x)\sqrt{|1-x|} \times \begin{cases} \ln\left|\frac{1+\sqrt{1-x}}{1-\sqrt{1-x}}\right| - i\pi & \text{for } x \equiv 4z^2/\hat{s} < 1 \\ 2\arctan\frac{1}{\sqrt{x-1}} & \text{for } x \equiv 4z^2/\hat{s} > 1 \end{cases},$$
$$g(0,\hat{s}) = \frac{8}{27} - \frac{8}{9}\ln\frac{m_b}{\mu} - \frac{4}{9}\ln\hat{s} + \frac{4}{9}i\pi \tag{2.8}$$

come from the one-loop contributions of the $\mathcal{O}_{1-6}$.

The $Y_{\rm res}$ term, which describes the long-distance contributions associated with the intermediate light vector mesons (such as ρ, ω, and ϕ) and vector charmonium states [such as J/ψ, $\psi(2S)$, etc.] (see the Fig. 1), is adopted as [57][1]

$$Y_{\rm res}(q^2,\mu) = -\frac{3\pi}{\alpha_e^2}\left[C(\mu)\sum_{V_i=J/\psi,\psi(2S),\ldots}\frac{m_{V_i}\mathcal{B}(V_i\to\ell^+\ell^-)\Gamma_{V_i}}{q^2-m_{V_i}^2+im_{V_i}\Gamma_{V_i}} - \lambda_u g(0,\hat{s})(3C_1(\mu)+C_2(\mu)) \times \sum_{V_j=\rho,\omega,\phi}\frac{m_{V_j}\mathcal{B}(V_j\to\ell^+\ell^-)\Gamma_{V_j}}{q^2-m_{V_j}^2+im_{V_j}\Gamma_{V_j}}\right], \tag{2.9}$$

where m_{V_i} and Γ_{V_i} are the mass and total width of the intermediate vector meson V_i respectively, and the $\Gamma(V_i\to\ell^+\ell^-)$ is the corresponding dilepton width. These input values are collected in Table I. In addition, the nonvanished branching fraction for the τ channel, i.e., $\mathcal{B}(\psi(2S)\to\tau^+\tau^-) = 3.1\times10^{-3}$ [188], is also used.

TABLE I. The masses, total widths and dilepton widths of the intermediate vector mesons used in Eq. (2.9). These values are quoted from the PDG [188].

V_i	m_{V_i} (GeV)	Γ_{V_i} (MeV)	$\mathcal{B}(V_i\to\ell^+\ell^-)$ where $\ell = e, \mu$
ρ	0.775	149	4.635×10^{-5}
ω	0.783	8.68	7.380×10^{-5}
ϕ	1.019	4.249	2.915×10^{-4}
J/ψ	3.097	0.093	5.966×10^{-2}
$\psi(2S)$	3.686	0.294	7.965×10^{-3}
$\psi(3770)$	3.774	27.2	9.6×10^{-6}
$\psi(4040)$	4.039	80	1.07×10^{-5}
$\psi(4160)$	4.191	70	6.9×10^{-6}

For the J/ψ and $\psi(2S)$ states, the small widths and the large dilepton width will have a large influence on the decay width. However, the narrow widths are also used to reject them in the experimental analysis. One the other hand, for those above the $D\bar{D}$ threshold, such as $\psi(3770)$, $\psi(4040)$, and $\psi(4160)$, the board widths and mutual overlap make things difficult. Also, for the charmless vector mesons (ρ, ω and ϕ), their contributions are suppressed by the λ_u factor.

B. The angular distributions and physical observables in the $B_c\to D_s^*(\to D_s\pi)\ell^+\ell^-$ decay

In this subsection, we will drive the formula of the quasi-four-body decay $B_c\to D_s^*(\to D_s\pi)\ell^+\ell^-$. The differential decay width of this process is

$$d\Gamma = \frac{|\mathcal{M}|^2}{2m_{B_c}}d\Phi_4(p;k_1,k_2,q_1,q_2), \tag{2.10}$$

where p is the four momentum of the initial B_c meson, $k_1(k_2)$ and $q_1(q_2)$ are the momenta of the mesons $D_s(\pi)$ and the lepton $\ell^-(\ell^+)$, respectively, and $d\Phi_4$ is the four-body phase space. Taking into account the width of the D_s^* meson, but treating it as narrow ($\Gamma_{D_s^*}\ll m_{D_s^*}$), the width can be obtained by doing the integration as

$$\int d\Phi_4\frac{|\mathcal{M}|^2}{2m_{B_c}}\xrightarrow{\Gamma_{D_s^*}\ll m_{D_s^*}}\frac{1}{2^{15}\pi^5 m_{B_c}m_{D_s^*}\Gamma_{D_s^*}}\int dq^2 d\cos\theta d\cos\theta_\ell d\phi\frac{\sqrt{\lambda(k^2,k_1^2,k_2^2)}}{k^2}\frac{\sqrt{\lambda(q^2,q_1^2,q_2^2)}}{q^2} \times\frac{\sqrt{\lambda(p^2,k^2,q^2)}}{p'^2}(k^2-m_{D_s^*}^2)^2|\mathcal{M}|^2\Big|_{k^2=m_{D_s^*}^2} \tag{2.11}$$

with $\lambda(x,y,z) = x^2+y^2+z^2-2(xy+xz+yz)$.

[1]This is a phenomenological method, and for more details on the charm-loop contribution, one can refer to Refs. [193–195].

The invariant amplitude $\mathcal{M}$ can be calculated from

$$\begin{aligned}\mathcal{M}(s_{\ell^+},s_{\ell^-}) &= \langle D_s\pi;\ell^+(s_{\ell^+})\ell^-(s_{\ell^-})|\mathcal{H}^{\rm eff}|B_c\rangle \\ &= \sum_{s_V}\frac{i}{k^2-m_{D_s^*}^2}\mathcal{M}_{D_s^*\to D_s\pi}(s_V)\langle D_s^*(s_V)\ell^+(s_{\ell^+})\ell^-(s_{\ell^-})|\mathcal{H}^{\rm eff}|B_c\rangle \\ &= \sum_{s_V}\frac{iN}{2(k^2-m_{D_s^*}^2)}\mathcal{M}_{D_s^*\to D_s\pi}(s_V)\Big\{C_9^{\rm eff}H^{V-A}(s_V,t)L^V(s_{\ell^+},s_{\ell^-},t)-\frac{2m_b}{q^2}C_7^{\rm eff}H^{T+T5}(s_V,t)L^V(s_{\ell^+},s_{\ell^-},t) \\ &\quad + C_{10}H^{V-A}(s_V,t)L^A(s_{\ell^+},s_{\ell^-},t)-\sum_{\lambda=\pm1,0}\Big[C_9^{\rm eff}H^{V-A}(s_V,\lambda)L^V(s_{\ell^+},s_{\ell^-},\lambda) \\ &\quad -\frac{2m_b}{q^2}C_7^{\rm eff}H^{T+T5}(s_V,\lambda)L^V(s_{\ell^+},s_{\ell^-},\lambda)+C_{10}H^{V-A}(s_V,\lambda)L^A(s_{\ell^+},s_{\ell^-},\lambda)\Big]\Big\},\end{aligned} \tag{2.12}$$

where $N=\frac{4G_F}{\sqrt{2}}V_{tb}V_{ts}^*\frac{\alpha_e}{4\pi}$, and the factor $1/2$ comes from the $P_{L(R)}$ in the effective Hamiltonian in Eq. (2.2).

For the amplitude $\mathcal{M}_{D_s^*\to D_s\pi}$, it can be evaluated by the effective Lagrangian approach. The concerned effective Lagrangian is

$$\mathcal{L}=g_{D_s^*D_s\pi}D_s^\dagger D_{s\mu}^*\partial^\mu\pi, \tag{2.13}$$

where $g_{D_s^*D_s\pi}$ is the corresponding coupling constant. So we have the decay width of $D_s^*\to D_s\pi$ as

$$\Gamma_{D_s^*}\times\mathcal{B}(D_s^*\to D_s\pi)=\frac{g_{D_s^*D_s\pi}^2}{48\pi}m_{D_s^*}\beta^3 \tag{2.14}$$

with $\beta=\sqrt{\lambda(m_{D_s^*}^2,m_{D_s}^2,m_\pi^2)}/m_{D_s^*}^2$. Obviously, the coupling constant $g_{D_s^*D_s\pi}$ can be canceled between the vertex factor and the decay width.

Finally, with the effective Hamiltonian in Eq. (2.2), we can calculate the quasi-four-body decay $B_c^-\to D_s^{*-}(\to D_s^-\pi^0)\ell^+\ell^-$. As deduced in Ref. [196], the corresponding angular distributions can be simplified as

$$\frac{d^4\Gamma}{dq^2d\cos\theta d\cos\theta_\ell d\phi}=\frac{9}{32\pi}\sum_i I_i(q^2)f_i(\theta,\theta_\ell,\phi), \tag{2.15}$$

where the explicit expressions of $I_i(q^2)$ and $f_i(\theta,\theta_\ell,\phi)$ are shown in Table II. Compared to Ref. [196], the term I_{6c} is neglected since it depends on the scalar operator. As shown in Fig. 2, the θ is the angle between the $-\hat{z}$ direction and pion-emitted direction in the rest frame of the D_s^* meson, the θ_ℓ is the angle made by the ℓ^- with the $+\hat{z}$ direction in the $\ell^+\ell^-$ center of mass system, and the ϕ is the angle between the decay planes, i.e., the $D_s^*\to D_s\pi$ plane and the virtual boson $\to\ell^+\ell^-$ plane.

The amplitudes $\mathcal{A}_{0,\parallel,\perp}^{L,R}$ and $\mathcal{A}_t$ are the functions of the transferred momentum square q^2, and the seven independent form factors V, $A_{0,1,2}$, and $T_{1,2,3}$, i.e., [57,58,196]

TABLE II. The explicit expressions of the angular coefficients I_i and f_i [57,58,196] in Eq. (2.15), where $\hat{m}_\ell^2=m_\ell^2/q^2$ and $\beta_\ell=\sqrt{1-4\hat{m}_\ell^2}$.

i	$I_i(q^2)$	$f_i(\theta,\theta_\ell,\phi)$
$1s$	$(\frac{3}{4}-\hat{m}_\ell^2)(\lvert\mathcal{A}_\parallel^L\rvert^2+\lvert\mathcal{A}_\perp^L\rvert^2+\lvert\mathcal{A}_\parallel^R\rvert^2+\lvert\mathcal{A}_\perp^R\rvert^2)+4\hat{m}_\ell^2\mathrm{Re}[\mathcal{A}_\perp^L\mathcal{A}_\perp^{R*}+\mathcal{A}_\parallel^L\mathcal{A}_\parallel^{R*}]$	$\sin^2\theta$
$1c$	$\lvert\mathcal{A}_0^L\rvert^2+\lvert\mathcal{A}_0^R\rvert^2+4\hat{m}_\ell^2(\lvert\mathcal{A}_t\rvert^2+2\mathrm{Re}[\mathcal{A}_0^L\mathcal{A}_0^{R*}])$	$\cos^2\theta$
$2s$	$\beta_\ell^2(\lvert\mathcal{A}_\parallel^L\rvert^2+\lvert\mathcal{A}_\perp^L\rvert^2+\lvert\mathcal{A}_\parallel^R\rvert^2+\lvert\mathcal{A}_\perp^R\rvert^2)/4$	$\sin^2\theta\cos2\theta_\ell$
$2c$	$-\beta_\ell^2(\lvert\mathcal{A}_0^L\rvert^2+\lvert\mathcal{A}_0^R\rvert^2)$	$\cos^2\theta\cos2\theta_\ell$
3	$\beta_\ell^2(\lvert\mathcal{A}_\perp^L\rvert^2-\lvert\mathcal{A}_\parallel^L\rvert^2+\lvert\mathcal{A}_\perp^R\rvert^2-\lvert\mathcal{A}_\parallel^R\rvert^2)/2$	$\sin^2\theta\sin^2\theta_\ell\cos2\phi$
4	$\beta_\ell^2\mathrm{Re}[\mathcal{A}_0^L\mathcal{A}_\parallel^{L*}+\mathcal{A}_0^R\mathcal{A}_\parallel^{R*}]/\sqrt{2}$	$\sin2\theta\sin2\theta_\ell\cos\phi$
5	$\sqrt{2}\beta_\ell\mathrm{Re}[\mathcal{A}_0^L\mathcal{A}_\perp^{L*}-\mathcal{A}_0^R\mathcal{A}_\perp^{R*}]$	$\sin2\theta\sin\theta_\ell\cos\phi$
$6s$	$2\beta_\ell\mathrm{Re}[\mathcal{A}_\parallel^L\mathcal{A}_\perp^{L*}-\mathcal{A}_\parallel^R\mathcal{A}_\perp^{R*}]$	$\sin^2\theta\cos\theta_\ell$
7	$\sqrt{2}\beta_\ell\mathrm{Im}[\mathcal{A}_0^L\mathcal{A}_\parallel^{L*}-\mathcal{A}_0^R\mathcal{A}_\parallel^{R*}]$	$\sin2\theta\sin\theta_\ell\sin\phi$
8	$\beta_\ell^2\mathrm{Im}[\mathcal{A}_0^L\mathcal{A}_\perp^{L*}+\mathcal{A}_0^R\mathcal{A}_\perp^{R*}]/\sqrt{2}$	$\sin2\theta\sin2\theta_\ell\sin\phi$
9	$\beta_\ell^2\mathrm{Im}[\mathcal{A}_\parallel^{L*}\mathcal{A}_\perp^L+\mathcal{A}_\parallel^{R*}\mathcal{A}_\perp^R]$	$\sin^2\theta\sin^2\theta_\ell\sin2\phi$

$$\mathcal{A}_{\perp}^{L,R}(q^2) = -N_{\ell}\sqrt{2N_{D_s^*}}\sqrt{\lambda(M'^2, M''^2, q^2)}\left[\left(C_9^{\rm eff} \mp C_{10}\right)\frac{V(q^2)}{M'+M''} + 2\hat{m}_b C_7^{\rm eff} T_1(q^2)\right],$$
$$\mathcal{A}_{\parallel}^{L,R}(q^2) = N_{\ell}\sqrt{2N_{D_s^*}}\left[\left(C_9^{\rm eff} \mp C_{10}\right)(M'+M'')A_1(q^2) + 2\hat{m}_b C_7^{\rm eff}\left(M'^2 - M''^2\right)T_2(q^2)\right],$$
$$\mathcal{A}_{0}^{L,R}(q^2) = \frac{N_{\ell}\sqrt{N_{D_s^*}}}{2M''\sqrt{q^2}}\left\{\left(C_9^{\rm eff} \mp C_{10}\right)\left[(M'^2 - M''^2 - q^2)(M'+M'')A_1(q^2) - \frac{\lambda(M'^2, M''^2, q^2)}{M'+M''}A_2(q^2)\right]\right.$$
$$\left. + 2m_b C_7^{\rm eff}\left[(M'^2 + 3M''^2 - q^2)T_2(q^2) - \frac{\lambda(M'^2, M''^2, q^2)}{M'^2 - M''^2}T_3(q^2)\right]\right\},$$
$$\mathcal{A}_{t}(q^2) = 2N_{\ell}\sqrt{N_{D_s^*}}\sqrt{\frac{\lambda(M'^2, M''^2, q^2)}{q^2}}C_{10}A_0(q^2), \tag{2.16}$$

where $M'(M'')$ is the mass of the B_c (D_s^*) meson and $\hat{m}_b = m_b/q^2$, and

$$N_{\ell} = \frac{i\alpha_e G_F}{4\sqrt{2}\pi}V_{tb}V_{ts}^*,$$
$$N_{D_s^*} = \frac{8\sqrt{\lambda}q^2}{3\times 256\pi^3 M'^3}\sqrt{1-\frac{4m_{\ell}^2}{q^2}}\mathcal{B}(D_s^* \to D_s\pi). \tag{2.17}$$

For the CP-conjugated mode $B_c^+ \to D_s^{*+}(\to D_s^+\pi^0)\ell^+\ell^-$, we have

$$\frac{d^4\bar{\Gamma}}{q^2 d\cos\theta d\cos\theta_{\ell} d\phi} = \sum_i \frac{9}{32\pi}\bar{I}_i(q^2)f_i(\theta,\theta_{\ell},\phi), \tag{2.18}$$

where $\bar{I}_i$ can be obtained by doing the conjugation for the weak phases of the CKM matrix elements in I_i in Table II. In addition, we should also do the following substitutions as

$$I_{1(c,s),2(c,s),3,4,7} \to \bar{I}_{1(c,s),2(c,s),3,4,7},$$
$$I_{5,6s,8,9} \to -\bar{I}_{5,6s,8,9}. \tag{2.19}$$

This is the result of the operations of $\theta_{\ell} \to \theta_{\ell} - \pi$ and $\phi \to -\phi$.

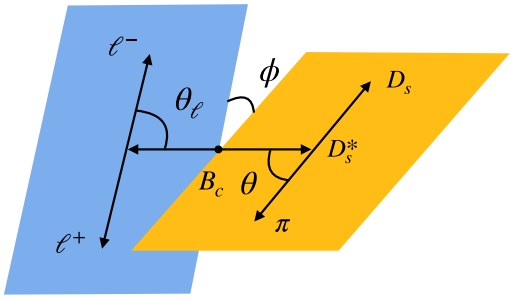

FIG. 2. Kinematics of the quasi-four-body decay $B_c \to D_s^*(\to D_s\pi)\ell^+\ell^-$.

To separate the CP-conserving and the CP-violating effects, we define the normalized CP-averaged angular coefficients S_i and the CP asymmetry angular coefficients A_i as

$$S_i = \frac{I_i + \bar{I}_i}{d(\Gamma+\bar{\Gamma})/dq^2},$$
$$A_i = \frac{I_i - \bar{I}_i}{d(\Gamma+\bar{\Gamma})/dq^2}, \tag{2.20}$$

respectively. To reduce both the experimental and theoretical uncertainties, the S_i and A_i have been normalized to the CP-averaged differential decay width. The other physical observables, such as the forward-backward asymmetry parameter $A_{\rm FB}$, the CP-violation $\mathcal{A}_{CP}$, and the longitudinal (transverse) polarization fractions of D_s^* meson $F_L(F_T)$, can thus be easily expressed in terms of these normalized angular coefficients. With the above preparations, we continue to study the physical observables.

(a) By integrating over the angles in the regions $\theta \in [0,\pi]$, $\theta_{\ell} \in [0,\pi]$, and $\phi \in [0,2\pi]$, the q^2-dependent differential decay width becomes

$$\frac{d\Gamma}{dq^2} = \frac{1}{4}(3I_{1c} + 6I_{1s} - I_{2c} - 2I_{2s}), \tag{2.21}$$

and that of the CP-conjugated mode $d\bar{\Gamma}/dq^2$ is analogous and can be obtained with the replacement in Eq. (2.19). So the CP-averaged differential decay width of $B_c \to D_s^*(\to D_s\pi)\ell^+\ell^-$ can be evaluated by

$$\frac{d\Gamma}{dq^2} = \frac{1}{2}\left(\frac{d\Gamma}{dq^2} + \frac{d\bar{\Gamma}}{dq^2}\right). \tag{2.22}$$

In this work, we focus on the CP-averaged decay width.

(b) The CP violation of the decay width can thus be estimated by

$$\mathcal{A}_{CP}(q^2) = \frac{(d\Gamma - d\bar{\Gamma})/dq^2}{(d\Gamma + d\bar{\Gamma})/dq^2} = \frac{1}{4}(3A_{1c} + 6A_{1s} - A_{2c} - 2A_{2s}). \tag{2.23}$$

(c) The CP asymmetry lepton forward-backward asymmetry is

$$A_{\rm FB}^{CP}(q^2) = \frac{(\int_{-1}^{0} - \int_{0}^{1}) d\cos\theta_\ell \int_{-1}^{1} d\cos\theta \int_{0}^{2\pi} d\phi \frac{d^4(\Gamma+\bar{\Gamma})}{dq^2 d\cos\theta d\cos\theta_\ell d\phi}}{d(\Gamma+\bar{\Gamma})/dq^2} = \frac{3}{4}A_6, \tag{2.24}$$

and the CP-averaged lepton forward-backward asymmetry is

$$A_{\rm FB}(q^2) = \frac{3}{4}S_6. \tag{2.25}$$

(d) The longitudinal and transverse D_s^* polarization fractions are

$$F_L = \frac{1}{4}(3S_{1c} - S_{2c}), \quad F_T = \frac{1}{2}(3S_{1s} - S_{2s}), \tag{2.26}$$

respectively.

Furthermore, the clean angular observables $P_{1,2,3}$ and $P'_{4,5,6,8}$ (more details can be found in Refs. [197,198]) are associated with the CP-averaged angular coefficients:

$$P_1 = \frac{S_3}{2S_{2s}}, \quad P_2 = \frac{\beta_\ell S_{6s}}{8S_{2s}}, \quad P_3 = -\frac{S_9}{4S_{2s}}, \tag{2.27}$$

$$P'_4 = \frac{S_4}{\sqrt{S_{1c}S_{2s}}}, \quad P'_5 = \frac{\beta_\ell S_5}{2\sqrt{S_{1c}S_{2s}}}, \quad P'_6 = -\frac{\beta_\ell S_7}{2\sqrt{S_{1c}S_{2s}}}, \quad P'_8 = -\frac{S_8}{\sqrt{S_{1c}S_{2s}}}. \tag{2.28}$$

As pointed out in Refs. [23,57,197,198], in the large-recoiled limit, these observables are largely free of form factor uncertainties.

Finally, we also focus on the ratios, i.e.,

$$R^{e\mu} = \frac{\int_{4m_\mu^2}^{(M'-M'')^2} \frac{d\Gamma[B_c\to D_s^*(\to D_s\pi)e^+e^-]}{dq^2} dq^2}{\int_{4m_\mu^2}^{(M'-M'')^2} \frac{d\Gamma[B_c\to D_s^*(\to D_s\pi)\mu^+\mu^-]}{dq^2} dq^2}, \quad R^{\tau\mu} = \frac{\int_{4m_\tau^2}^{(M'-M'')^2} \frac{d\Gamma[B_c\to D_s^*(\to D_s\pi)\tau^+\tau^-]}{dq^2} dq^2}{\int_{4m_\mu^2}^{(M'-M'')^2} \frac{d\Gamma[B_c\to D_s^*(\to D_s\pi)\mu^+\mu^-]}{dq^2} dq^2}, \tag{2.29}$$

which reflect the LFU. We would like to emphasize that the lower limit of the integral of the electron mode is chosen as $4m_\mu^2$ instead of the kinematic limit $4m_e^2$ in order to exclude the large enhancement dominated by the photon pole in the small q^2 region due to the $C_7^{\rm eff}$-associated factor $1/q^2$. In the $B \to K\ell^+\ell^-$ process, the experimental measurements of the ratio $R_K^{e\mu}$ by Belle [9–12] and *BABAR* [15] are in agreement with the SM prediction, while the LHCb result [19,21,22] shows a clear deviation from the SM expectation (see Fig. 4 of Ref. [22]) with 3.1σ. We note that in Ref. [199], the authors used the ratios $R_{K^{(*)}}^{\tau\mu}$ to study the LFU violation, and found that they can deviate from the SM prediction even if the NP couplings are universal. Therefore, in order to use these ratios to study the LFU violation, we should compare the allowed ranges, considering both the solutions with only universal couplings and those with universal and nonuniversal components. Whatever, the ratio in the $B_c \to D_s^*\ell^+\ell^-$ sector is also interesting to investigate whether it is consistent with the SM expectation or not. The breaking of the LFU may require an expansion of the gauge structure of the SM, and of course probes the NP effects [200].

III. WEAK TRANSITION FORM FACTORS

The standard and(or) covariant LFQMs have been widely used to study the decays of mesons [118–156] and baryons [158–185]. In the conventional LFQM framework, the consistent quark (or antiquark) of the meson is required to be on its mass shell, and thus the initial (or final) meson is off shell. This procedure misses the zero-mode effects and makes the matrix element noncovariant. To avoid this shortcoming, Jaus [118,122] proposed a covariant framework for the S-waved pseudoscalar and vector meson decays in which the zero-mode contributions are systematically taken into account. Cheng *et al.* [124,132] extended this approach to the case of the P-wave meson (such as scalar, axial-vector and tensor mesons). The physical quantities, such as the decay constant and the form factor of the weak transition, are obtained in terms of the Feynman loop integration. Unlike the conventional LFQM, the covariant LFQM requires the initial (or final) meson to be on its mass shell. For more details on the difference, see Refs. [124,146]. In this section, we will use the covariant LFQM to calculate the $B_c \to D_s^*$ form factors.

Following Ref. [154], the $B_c \to D_s^*$ weak transition form factors deduced by (axial-)vector currents are defined as

$$\begin{aligned}\langle D_s^*(p'')|\bar{s}\gamma_\mu b|B_c(p')\rangle &= \epsilon_{\mu\nu\alpha\beta}\varepsilon^{*\nu}P^\alpha q^\beta g(q^2),\\ \langle D_s^*(p'')|\bar{s}\gamma_\mu\gamma_5 b|B_c(p')\rangle &= -i\Big\{\varepsilon_\mu^* f(q^2)+\varepsilon^*\cdot P(P_\mu a_+(q^2)+q_\mu a_-(q^2))\Big\},\end{aligned} \tag{3.1}$$

where we use the convention $\epsilon_{0123}=+1$ and define $P_\mu = p'_\mu + p''_\mu$ and $q_\mu = p'_\mu - p''_\mu$, and ε is the polarization vector of the D_s^* meson. These amplitudes can also be parametrized as the Bauer-Stech-Wirbel (BSW) form [201], i.e.,

$$\begin{aligned}\langle D_s^*(p'')|\bar{s}\gamma_\mu b|B_c(p')\rangle &= -\frac{1}{M'+M''}\epsilon_{\mu\nu\alpha\beta}\varepsilon^{*\nu}P^\alpha q^\beta V(q^2),\\ \langle D_s^*(p'')|\bar{s}\gamma_\mu\gamma_5 b|B_c(p')\rangle &= i\Big\{(M'+M'')\varepsilon_\mu^* A_1(q^2)-\frac{\varepsilon^*\cdot P}{M'+M''}P_\mu A_2(q^2)-2M''\frac{\varepsilon^*\cdot P}{q^2}q_\mu\Big[A_3(q^2)-A_0(q^2)\Big]\Big\}\end{aligned} \tag{3.2}$$

with $M'(M'')$ being the mass of the parent (daughter) meson. These two definitions are related by the relations [154]

$$\begin{aligned}&V(q^2)=-(M'+M'')g(q^2), \qquad A_1(q^2)=-\frac{f(q^2)}{M'+M''},\\ &A_2(q^2)=(M'+M'')a_+(q^2), \qquad A_3(q^2)-A_0(q^2)=\frac{q^2}{2M''}a_-(q^2),\\ &A_3(q^2)=\frac{M'+M''}{2M''}A_1(q^2)-\frac{M'-M''}{2M''}A_2(q^2).\end{aligned} \tag{3.3}$$

In addition, the (pseudo)tensor current amplitudes can be defined as [202,203]

$$\begin{aligned}\langle D_s^*(p'')|\bar{s}i\sigma_{\mu\nu}q^\nu b|B_c(p')\rangle &= T_1(q^2)\epsilon_{\mu\nu\alpha\beta}\varepsilon^{*\nu}P^\alpha q^\beta,\\ \langle D_s^*(p'')|\bar{s}i\sigma_{\mu\nu}q^\nu\gamma_5 b|B_c(p')\rangle &= iT_2(q^2)\Big[(M'^2-M''^2)\varepsilon_\mu^*-\varepsilon^*\cdot qP_\mu\Big]+iT_3(q^2)\varepsilon^*\cdot q\Big[q_\mu-\frac{q^2}{M'^2-M''^2}P_\mu\Big],\end{aligned} \tag{3.4}$$

where we have $T_1(0)=T_2(0)$ since the identity $2\sigma_{\mu\nu}\gamma_5 = -i\epsilon_{\mu\nu\alpha\beta}\sigma^{\alpha\beta}$.

The form factors require a nonperturbative calculation. In this work, we use the covariant LFQM to calculate the relevant form factors for the weak transition. In this approach, the constituent quark and the antiquark inside a meson are off shell. We define the incoming (outgoing) meson to have the momentum $P'=p'_1+p_2(P''=p''_1+p_2)$, where $p_1^{\prime(\prime\prime)}$ and p_2 are the off-shell momenta of the quark and the antiquark, respectively. These momenta can be expressed in terms of the internal variables $(x_i,\vec{k}'_\perp)$ $(i=1,2)$, defined by

$$p_1'^+ = x_1 P'^+, \qquad p_1^+ = x_2 P'^+, \qquad \vec{p}'_{1\perp} = x_1\vec{P}'_\perp + \vec{k}'_\perp. \tag{3.5}$$

They must also satisfy $x_1+x_2=1$.

According to Refs. [124,154], the corresponding weak transition matrix element at the one-loop level can be calculated in terms of the Feynman loop integral, as shown in Fig. 3. Then the form factors can be extracted from the

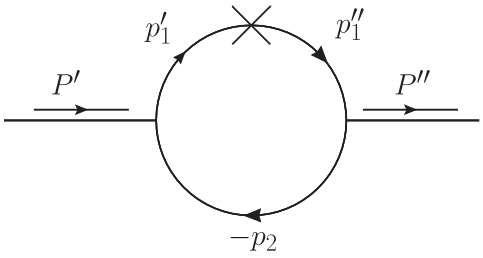

FIG. 3. The one-loop Feynman diagram for meson weak transition amplitude, where $P'(P'')$ is the momentum of the incoming (outgoing) meson, $p_1^{\prime(\prime\prime)}$ and p_2 are the momenta of the quark and antiquark, respectively. The symbol "cross" denotes the weak interaction vertex.

corresponding matrix element. To write down the transition amplitude, we need the meson-quark antiquark vertices for the initial meson as $i\Gamma' = H'_P\gamma_5$, and that of the outgoing meson as $i(\gamma_0\Gamma''^{\dagger}\gamma_0)$ with $\Gamma'' = H''_V[\gamma_\mu - (p''_1 - p_2)_\mu/W''_V]$ [124,154], where the subscripts P and V denote the pseudoscalar and vector meson, respectively.

For Fig. 3, the concrete expression of the transition amplitude for $P \to V$ can be expressed as

$$\mathcal{B}_\mu^{V(A,T,T5)} = -i^3\frac{N_c}{(2\pi)^4}\int d^4p'_1\frac{iH'_PH''_V}{N'_1N''_1N_2}S_{\mu\nu}^{V(A,T,T5)}\epsilon_V^{*\nu}, \quad (3.6)$$

where $N_1^{\prime(\prime\prime)} = p_1^{\prime(\prime\prime)2} - m_1^{\prime(\prime\prime)2}$ and $N_2 = p_2^2 - m_2^2$ come from the propagators of the quarks. The superscripts V, A, T, and $T5$ represent the vector, axial-vector, tensor, and pseudotensor currents, respectively. The traces $S_{\mu\nu}^V$ are written as

$$\begin{aligned}S_{\mu\nu}^V &= \mathrm{Tr}\left[\left(\gamma_\nu - \frac{(p''_1 - p_2)_\nu}{W''_V}\right)(\not{p}''_1 + m''_1)\gamma_\mu\right.\\ &\quad\left.\times(\not{p}'_1 + m'_1)\gamma_5(-\not{p}_2 + m_2)\right]\\ &= -2i\epsilon_{\mu\nu\alpha\beta}\left[p_1'^\alpha P^\beta(m''_1 - m'_1) + p_1'^\alpha q^\beta(m''_1 + m'_1 - 2m_2)\right.\\ &\quad\left. + q^\alpha P^\beta m'_1\right] + \frac{1}{W''_V}(4p'_{1\nu} - 3q_\nu - P_\nu)i\epsilon_{\mu\alpha\beta\rho}p_1'^\alpha q^\beta P^\rho.\end{aligned} \quad (3.7)$$

To make reading easier, the relevant expressions of the traces $S_{\mu\nu}^{A,T,T5}$ are collected in the Appendix.

Following Refs. [123,124,132], the execution of the $p_1'^-$ integration went to the replacement:

$$\begin{aligned}N_1^{\prime(\prime\prime)} &\to \hat{N}_1^{\prime(\prime\prime)} = x_1(M'^{(\prime\prime)2} - M_0^{\prime(\prime\prime)2}),\\ H_{P(V)}^{\prime(\prime\prime)} &\to h_{P(V)}^{\prime(\prime\prime)},\\ W''_V &\to \omega''_V,\\ \int\frac{d^4p'_1}{(2\pi)^4}H'_PH''_VS_{\mu\nu}\epsilon^{*\nu} &\to -i\pi\int\frac{dx_2d^2\vec{k}'_\perp}{x_2\hat{N}'_1\hat{N}''_1}h'_Ph''_V\hat{S}_{\mu\nu}\epsilon^{*\nu},\end{aligned} \quad (3.8)$$

where we define

$$M_0^{\prime(\prime\prime)2} = \frac{\vec{k}_\perp^{\prime(\prime\prime)2} + m_1^{\prime(\prime\prime)2}}{x_1} + \frac{\vec{k}_\perp^{\prime(\prime\prime)2} + m_2^{\prime(\prime\prime)2}}{x_2}, \quad (3.9)$$

with $\vec{k}''_\perp = \vec{k}'_\perp - x_2\vec{q}_\perp$ and $\omega''_V = M''_0 + m''_1 + m_2$.

To write down the concrete expression of $\hat{S}_{\mu\nu}$, we should take into account the so-called zero-mode contribution. As shown in Refs. [124,141], after doing the integration in Eq. (3.8) we have $p_2 = \hat{p}_2$, and

$$\begin{aligned}\hat{p}_1'^\mu &= (P' - \hat{p}_2)^\mu\\ &= x_1P'^\mu + (0,0,\vec{k}'_\perp)^\mu + \frac{1}{2}\left(x_2P'^- - \frac{\vec{p}_{2\perp}^2 + m_2^2}{x_2P'^+}\right)\tilde{\omega}^\mu,\end{aligned} \quad (3.10)$$

where $\tilde{\omega} = (2,0,\vec{0}_\perp)$ is a lightlike four vector in the light-front coordinate. Following the discussions in a series of papers [123,124,132,141], for avoiding the $\tilde{\omega}$ dependence, we need to do the following replacements [123,124,132]:

$$\begin{aligned}\hat{p}'_{1\mu} &\doteq P_\mu A_1^{(1)} + q_\mu A_2^{(1)},\\ \hat{p}'_{1\mu}\hat{p}'_{1\nu} &\doteq g_{\mu\nu}A_1^{(2)} + P_\mu P_\nu A_2^{(2)} + (P_\mu q_\nu + P_\nu q_\mu)A_3^{(2)} + q_\mu q_\nu A_4^{(2)},\\ N_2 &\doteq Z_2,\\ \hat{p}'_{1\mu}\hat{N}_2 &\doteq q_\mu\left(A_2^{(1)}Z_2 + \frac{P\cdot q}{q^2}A_1^{(2)}\right),\\ \hat{p}'_{1\mu}\hat{p}'_{1\nu}\hat{N}_2 &\doteq g_{\mu\nu}A_1^{(2)}Z_2 + q_\mu q_\nu\left[A_4^{(2)}Z_2 + 2\frac{P\cdot q}{q^2}A_2^{(1)}A_1^{(2)}\right],\end{aligned} \quad (3.11)$$

in Eqs. (3.7), (A1), (A4), and (A5). Here, $Z_2 = \hat{N}'_1 + m'^2_1 - m_2^2 + (1-2x_1)M'^2 + (q^2 + P\cdot q)\frac{\vec{k}'_\perp\cdot\vec{q}_\perp}{q^2}$, $P\cdot q = M'^2 - M''^2$, and

$$
\begin{aligned}
&A_1^{(1)} = \frac{x_1}{2}, \qquad A_2^{(1)} = A_1^{(1)} - \frac{\vec{k}'_\perp\cdot\vec{q}_\perp}{q^2},\\
&A_1^{(2)} = -\vec{k}'^2_\perp - \frac{(\vec{k}'_\perp\cdot\vec{q}_\perp)^2}{q^2}, \qquad A_2^{(2)} = (A_1^{(1)})^2,\\
&A_3^{(2)} = A_1^{(1)}A_2^{(1)}, \qquad A_4^{(2)} = (A_2^{(1)})^2 - \frac{1}{q^2}A_1^{(2)}.
\end{aligned}
\tag{3.12}
$$

After performing the replacements (3.11) in the decay amplitudes (3.7) and (A1), the form factors g, f, a_+, and a_- can be obtained from the terms proportional to the $\epsilon_{\mu\nu\alpha\beta}P^\alpha q^\beta$, $g_{\mu\nu}$, $P_\mu P_\nu$, and $P_\mu q_\nu$, and $q_\mu P_\nu$ and $q_\mu q_\nu$, respectively. The $\epsilon_V^{*\mu}P''_\mu = 0$ is used here. Finally, the expressions of these form factors in covariant LFQMs can be written as [122,124,154]

$$
g(q^2) = -\frac{N_c}{16\pi^3}\int dx_2 d^2\vec{k}_{2\perp}\frac{2h'_P h''_V}{x_2\hat{N}'_1\hat{N}''_1}\left\{x_2 m'_1 + x_1 m_2 + (m'_1 - m''_1)\frac{k'_\perp\cdot q_\perp}{q^2} + \frac{2}{\omega''_V}\left[k'^2_\perp + \frac{(k'_\perp\cdot q_\perp)^2}{q^2}\right]\right\},
\tag{3.13}
$$

$$
\begin{aligned}
f(q^2) = \frac{N_c}{16\pi^3}\int dx_2 d^2\vec{k}'_\perp \frac{h'_P h''_V}{x_2\hat{N}'_1\hat{N}''_1}\Big\{&2x_1(m_2 - m'_1)(M'^2_0 + M''^2_0) - 4x_1 m''_1 M'^2_0 + 2x_2 m'_1 P\cdot q + 2m_2 q^2\\
&- 2x_1 m_2(M'^2 + M''^2) + 2(m'_1 - m_2)(m'_1 + m''_1)^2 + 8(m'_1 - m_2)\left[k'^2_\perp + \frac{(k'_\perp\cdot q_\perp)^2}{q^2}\right]\\
&+ 2(m'_1 + m''_1)(q^2 + P\cdot q)\frac{k'_\perp\cdot q_\perp}{q^2} - 4\frac{q^2 k'^2_\perp + (k'_\perp\cdot q_\perp)^2}{q^2\omega''_V}\Big[2x_1(M'^2 + M'^2_0) - q^2 - P\cdot q\\
&- 2(q^2 + P\cdot q)\frac{k'_\perp\cdot q_\perp}{q^2} - 2(m'_1 - m''_1)(m'_1 - m_2)\Big]\Big\},
\end{aligned}
\tag{3.14}
$$

$$
\begin{aligned}
a_+(q^2) = \frac{N_c}{16\pi^3}\int dx_2 d^2\vec{k}'_\perp \frac{2h'_P h''_V}{x_2\hat{N}'_1\hat{N}''_1}\Big\{&(x_1 - x_2)(x_2 m'_1 + x_1 m_2) - [2x_1 m_2 + m''_1 + (x_2 - x_1)m'_1]\frac{k'_\perp\cdot q_\perp}{q^2}\\
&- 2\frac{x_2 q^2 + k'_\perp\cdot q_\perp}{x_2 q^2\omega''_V}[k'_\perp\cdot k''_\perp + (x_1 m_2 + x_2 m'_1)(x_1 m_2 - x_2 m''_1)]\Big\},
\end{aligned}
\tag{3.15}
$$

$$
\begin{aligned}
a_-(q^2) = \frac{N_c}{16\pi^3}\int dx_2 d^2\vec{k}'_\perp \frac{h'_P h''_V}{x_2\hat{N}'_1\hat{N}''_1}\Big\{&2(2x_1 - 3)(x_2 m'_1 + x_1 m_2) - 8(m'_1 - m_2)\left[\frac{k'^2_\perp}{q^2} + 2\frac{(k'_\perp\cdot q_\perp)^2}{q^4}\right]\\
&- [(14 - 12x_1)m'_1 - 2m''_1 - (8 - 12x_1)m_2]\frac{k'_\perp\cdot q_\perp}{q^2} + \frac{4}{\omega''_V}\Big([M'^2 + M''^2 - q^2 + 2(m'_1 - m_2)(m''_1 + m_2)]\\
&\times(A_3^2 + A_4^{(2)} - A_2^1) + Z_2(3A_2^{(1)} - 2A_4^{(2)} - 1) + \frac{1}{2}P\cdot q(A_1^{(1)} + A_2^{(1)} - 1)[x_1(q^2 + P\cdot q) - 2M'^2 - 2k'_\perp\cdot q_\perp\\
&- 2m'_1(m''_1 + m_2 - 2m_2(m'_1 - m_2))]\left[\frac{k'^2_\perp}{q^2} + \frac{(k'_\perp\cdot q_\perp)^2}{q^4}\right](4A_2^{(1)} - 3)\Big)\Big\}.
\end{aligned}
\tag{3.16}
$$

The form factors deduced by (axial) vector currents defined in Eq. (3.2) can thus be evaluated by

$$
\begin{aligned}
&V(q^2) = -(M' + M'')g(q^2),\\
&A_0(q^2) = -\frac{1}{2M''}f(q^2) - \frac{M'^2 - M''^2}{2M''}a_+(q^2) - \frac{q^2}{2M''}a_-(q^2),\\
&A_1(q^2) = -f(q^2)/(M' + M''), \qquad A_2(q^2) = (M' + M'')a_+(q^2).
\end{aligned}
\tag{3.17}
$$

Analogously, we can obtain the concrete expressions of the (pseudo)tensor form factors defined in Eq. (3.4) as [132]

$$T_1(q^2) = \frac{N_c}{16\pi^3}\int dx_2 d^2\vec{k}'_\perp \frac{h'_P h''_V}{x_2\hat{N}'_1\hat{N}''_1}\Big\{2A_1^{(1)}[M'^2 - M''^2 - 2m_1'^2 - 2\hat{N}'_1 + q^2 + 2(m'_1 m_2 + m''_1 m_2 - m'_1 m''_1)]$$
$$- 8A_1^{(2)} + (m'_1 + m''_1)^2 + \hat{N}'_1 + \hat{N}''_1 - q^2 + 4(M'^2 - M''^2)(A_2^{(2)} - A_3^{(2)}) + 4q^2(-A_1^{(1)} + A_2^{(1)} + A_3^{(2)} - A_4^{(2)})$$
$$- \frac{4}{\omega''_V}(m'_1 + m''_1)A_1^{(2)}\Big\}, \tag{3.18}$$

$$T_2(q^2) = T_1(q^2) + \frac{q^2}{M'^2 - M''^2}\frac{N_c}{16\pi^3}\int dx_2 d^2\vec{k}'_\perp \frac{h'_P h''_V}{x_2\hat{N}'_1\hat{N}''_1}\Big\{2A_2^{(1)}[M'^2 - M''^2 - 2m_1'^2 - 2\hat{N}'_1 + q^2$$
$$+ 2(m'_1 m_2 + m''_1 m_2 - m'_1 m''_1)] - 8A_1^{(2)} - 2M'^2 + 2m_1'^2 + (m'_1 + m''_1)^2 + 2(m_2 - 2m'_1)m_2 + 3\hat{N}'_1 + \hat{N}''_1$$
$$- q^2 + 2Z_2 + 4(q^2 - 2M'^2 - 2M''^2)(A_2^{(2)} - A_3^{(2)}) - 4(M'^2 - M''^2)(-A_1^{(1)} + A_2^{(1)} + A_3^{(2)} - A_4^{(2)})$$
$$- \frac{4}{\omega''_V}(m''_1 - m'_1 + 2m_2)A_1^{(2)}\Big\}, \tag{3.19}$$

$$T_3(q^2) = \frac{N_c}{16\pi^3}\int dx_2 d^2\vec{k}'_\perp \frac{h'_P h''_V}{x_2\hat{N}'_1\hat{N}''_1}\Big\{-2A_2^{(1)}[M'^2 - M''^2 - 2m_1'^2 - 2\hat{N}'_1 + q^2 + 2(m'_1 m_2 + m''_1 m_2 - m'_1 m''_1)]$$
$$+ 8A_1^{(2)} + 2M'^2 - 2m_1'^2 - (m'_1 + m''_1)^2 - 2(m_2 - 2m'_1)m_2 - 3\hat{N}'_1 - \hat{N}''_1 + q^2 - 2Z_2 - 4(q^2 - M'^2 - 3M''^2)$$
$$\times (A_2^{(2)} - A_3^{(2)}) + \frac{4}{\omega''_V}\Big((m''_1 - m'_1 + 2m_2)[A_1^{(2)} + (M'^2 - M''^2)(A_2^{(2)} + A_3^{(2)} - A_1^{(1)})]$$
$$+ (m'_1 + m''_1)(M'^2 - M''^2)(A_2^{(1)} - A_3^{(2)} - A_4^{(2)}) + m'_1(M'^2 - M''^2)(A_1^{(1)} + A_2^{(1)} - 1)\Big)\Big\}. \tag{3.20}$$

Following the treatment in Ref. [124], h_M is taken as

$$h'_P = (M'^2 - M_0'^2)\sqrt{\frac{x_1x_2}{N_c}}\frac{1}{\sqrt{2}\tilde{M}'_0}\phi_s(x_2,\vec{k}'_\perp),$$
$$h''_V = (M''^2 - M_0''^2)\sqrt{\frac{x_1x_2}{N_c}}\frac{1}{\sqrt{2}\tilde{M}''_0}\phi_s(x_2,\vec{k}''_\perp), \tag{3.21}$$

where $\tilde{M}_0^{\prime(\prime\prime)} = \sqrt{M_0^{\prime(\prime\prime)2} - (m_1^{\prime(\prime\prime)} - m_2)^2}$, and ϕ_s is the space wave function of the pseudoscalar or vector meson.

In the previous theoretical work [124,154], the phenomenological Gaussian-type wave functions

$$\phi_s(x_2,\vec{k}_\perp^{\prime(\prime\prime)}) = 4\left(\frac{\pi}{\beta^{\prime(\prime\prime)2}}\right)^{3/4}\sqrt{\frac{e_1^{\prime(\prime\prime)}e_2}{x_1x_2M_0^{\prime(\prime\prime)}}}$$
$$\times\exp\left(-\frac{\vec{k}_\perp^{\prime(\prime\prime)2} + k_z^{\prime(\prime\prime)2}}{2\beta^{\prime(\prime\prime)2}}\right), \tag{3.22}$$

with

$$k_z^{\prime(\prime\prime)} = \frac{x_2M_0^{\prime(\prime\prime)}}{2} - \frac{m_2^2 + \vec{k}_\perp^{\prime(\prime\prime)2}}{2x_2M_0^{\prime(\prime\prime)}},$$
$$e_1^{\prime(\prime\prime)} = \sqrt{m_1^{\prime(\prime\prime)2} + \vec{k}_\perp^{\prime(\prime\prime)2} + k_z^{\prime(\prime\prime)2}},$$
$$e_2 = \sqrt{m_2^2 + \vec{k}_\perp'^2 + k_z'^2}, \tag{3.23}$$

are widely used. It inevitably introduces the dependence of the parameter β. The phenomenological parameter β can be fixed by the decay constant [123,124,132]. However, as we all know, the decay constant is only associated with the meson wave function at the end point $q^2 = 0$. This indicates that the simple wave function Eq. (3.22) deviating from the $q^2 = 0$ region may be unreliable.

Taking advantage of the modified GI model [204], we can obtain the numerical spatial wave functions of the mesons concerned. By replacing the form in Eq. (3.22) with

TABLE III. The calculated masses and the expansion coefficients c_n of the wave function of the mesons involved [204]. The masses are given in units of MeV.

States	Masses [204]	Experiments [188]	Eigenvector coefficients c_n [204]
B_c	6271	6274.47 ± 0.32	{0.7877, 0.4410, 0.2857, 0.1991, 0.1470, 0.1132, 0.0900, 0.0734, 0.0611, 0.0517, 0.0444, 0.0385, 0.0338, 0.0299, 0.0266, 0.0238, 0.0215, 0.0195, 0.0177, 0.0162, 0.0148, 0.0136, 0.0125, 0.0116, 0.0107, 0.0099, 0.0092, 0.0084, 0.0081, 0.0066, 0.0081}
D_s^*	2112	2112.2 ± 0.4	{0.9708, 0.16203, 0.1515, 0.0605, 0.0518, 0.0286, 0.0240, 0.0156, 0.0130, 0.0093, 0.0078, 0.0059, 0.0050, 0.0039, 0.0033, 0.0027, 0.0023, 0.0019, 0.0016, 0.0013 0.0012, 0.0010, 0.0008, 0.0007, 0.0006, 0.0005, 0.0005, 0.0004, 0.0003, 0.0003, 0.0003}

$$\phi_l(x_2,\vec{k}_\perp^{\prime(\prime\prime)}) = \sqrt{4\pi}\sum_{n=1}^{N_{\max}} c_n \sqrt{\frac{e_1^{\prime(\prime\prime)} e_2}{x_1 x_2 M_0^{\prime(\prime\prime)}}} R_{nl} \times \left(\sqrt{\vec{k}_\perp^{\prime(\prime\prime)2} + k_z^{\prime(\prime\prime)2}}\right),$$
$$\phi_s(x_2,\vec{k}_\perp^{\prime(\prime\prime)}) \equiv \phi_{l=0}(x_2,\vec{k}_\perp^{\prime(\prime\prime)}), \tag{3.24}$$

where c_n are the expansion coefficients of the corresponding eigenvectors and l is the orbital angular momentum of the meson, we can avoid the corresponding uncertainty. In Table III, we collect the expansion coefficients c_n of the meson wave functions involved. In addition, the factor $\sqrt{4\pi}$ is needed to satisfy the normalization:

$$\int \frac{dx_2 d\vec{k}_\perp}{2(2\pi)^3} \phi_l^*(x_2,\vec{k}_\perp)\phi_l(x_2,\vec{k}_\perp) = 1. \tag{3.25}$$

Besides, the R_{nl} is the simple harmonic oscillator wave function as

$$R_{nl}(|p|) = \frac{(-1)^{n-1}}{\beta^{3/2}} \sqrt{\frac{2(n-1)!}{\Gamma(n+l+1/2)}} \left(\frac{p}{\beta}\right)^l \times \exp\left(-\frac{p^2}{2\beta^2}\right) L_{n-1}^l\left(\frac{p^2}{\beta^2}\right). \tag{3.26}$$

The parameter $\beta = 0.5$ GeV in the above equation is consistent with Ref. [204].

IV. NUMERICAL RESULTS AND DISCUSSIONS

A. The form factors

With the input of the numerical wave functions, and the concrete expressions of the seven form factors in Eqs. (3.13)–(3.20), we present in this subsection the numerical results of $B_c \to D_s^*$ form factors.

Following the approach described in Refs. [122,124], we assume the condition $q^+ = 0$. This implies that our form factor calculations are performed in the spacelike region ($q^2 < 0$), and therefore we need to extrapolate them to the timelike region ($q^2 > 0$). To perform the analytical continuation, we utilize the z-series parametrization [141]

$$\mathcal{F}(q^2) = \frac{\mathcal{F}(0)}{1 - q^2/m_{\text{pole}}^2}\left\{1 + a_1\left(z(q^2) - z(0) - \frac{1}{3}\left[z(q^2)^2 - z(0)^2\right]\right) + a_2\left(z(q^2) - z(0) + \frac{2}{3}\left[z(q^2)^2 - z(0)^2\right]\right)\right\}, \tag{4.1}$$

where a_i ($i = 1, 2$) are free parameters needed to fit in the $q^2 < 0$ region, and the $z(q^2)$ is taken as

$$z(q^2) = \frac{\sqrt{t_+ - q^2} - \sqrt{t_+ - t_0}}{\sqrt{t_+ - q^2} + \sqrt{t_+ - t_0}} \tag{4.2}$$

with $t_\pm = (M' \pm M'')^2$ and $t_0 = t_+\left(1 - \sqrt{1 - t_-/t_+}\right)$.

To determine the values of the free parameters a_i, as given in Eq. (4.1), we perform numerical calculations at 200 equally spaced points for each form factor, ranging from -20 to -0.1 GeV^2, using Eqs. (3.13)–(3.20). The calculated points are then fitted using Eq. (4.1). The fitted values of the free parameters, as well as $\mathcal{F}(0)$, $\mathcal{F}(q^2_{\max})$, and the pole masses, are listed in Table IV. Additionally, the q^2 dependence of the transition form factors $B_c \to D_s^*$ is shown in Fig. 4.

In Table V, we compare our results for the $B_c \to D_s^*$ weak transition form factors at the end point $q^2 = 0$ with other approaches, in which Refs. [113,114] calculated the concerned form factors with the QCD sum rule,

TABLE IV. Our results of the weak transition form factors of $B_c \to D_s^*$ by using the covariant LFQM.

	$\mathcal{F}(0)$	$\mathcal{F}(q^2_{\max})$	m_{pole} (GeV)	a_1	a_2
$V^{B_c\to B_s^*}$	0.434	1.652	5.415	−7.909	15.667
$A_0^{B_c\to B_s^*}$	0.387	1.436	5.367	−6.790	9.427
$A_1^{B_c\to B_s^*}$	0.274	0.588	5.829	−0.721	−4.299
$A_2^{B_c\to B_s^*}$	0.159	0.438	5.829	−4.942	5.168
$T_1^{B_c\to B_s^*}$	0.265	1.050	5.415	−8.821	19.272
$T_2^{B_c\to B_s^*}$	0.265	0.424	5.829	3.067	−9.950
$T_3^{B_c\to B_s^*}$	0.231	0.637	5.829	−4.985	4.566

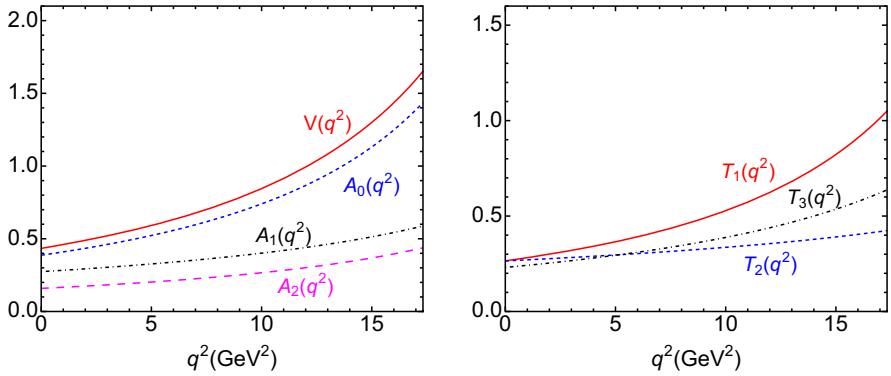

FIG. 4. The q^2 dependence of the $B_c \to D_s^*$ weak transition form factors. Here, the four dependent form factors deduced by (axial) vector are presented in the left panel, while the three dependent ones deduced by (pseudo)tensor are shown in the right panel.

Refs. [112,128,154] used the covariant LFQM, and Ref. [205] used the Bauer-Stech-Wirbel model and considered the effects of flavor dependence on the form factors caused by possible variation of the average transverse quark momentum (ω) inside the meson. In addition, Ref. [112] also used the CQM, and Ref. [111] used the pQCD approach. References [111,112,114] contain the results of (pseudo)tensor form factors. Obviously, our results of the (pseudo)tensor form factors, i.e., $T_{1,2,3}$, at the end point $q^2 = 0$ are consistent with the predictions of pQCD [111] and the LFQM [112]. We expect further theoretical work, especially LQCD, which is useful to constrain the behavior of the form factors in the low-recoiling region, to test our results.

B. The angular distributions and physical observables

With the above preparations, in this subsection we present our numerical results of the branching fractions and some angular observables, i.e., the CP-averaged normalized angular coefficients S_i, the lepton's forward-backward asymmetry parameter $A_{\rm FB}$, and the longitudinal (transverse) polarization fractions of the D_s^* meson $F_{L(T)}$. In addition, we also investigate the clean angular observables $P_{1,2,3}$ and $P'_{4,5,6,8}$. The hadron and lepton masses are quoted from the PDG [188], as well as the lifetime $\tau_{B_c} = 0.510$ ps and the branching fraction $\mathcal{B}(D_s^* \to D_s\pi) = 5\%$.

First, we focus on the angular coefficients S_i and A_i defined in Eq. (2.20). The q^2 dependence of the normalized CP-averaged angular coefficients S_i are presented in Fig. 5, while the CP asymmetry angular coefficients A_i are shown in Fig. 6. The blue dashed lines and the magenta solid lines represent the muon and the tau channels, respectively. Since the electron channel shows similar behavior to the muon channel, we will only present our results for the muon and the tau channels here. In the energy regions of $8.0 < q^2 < 11.0$ and $12.5 < q^2 < 15.0$ GeV^2, we use the gray areas to mark the contributions from the charmonium states J/ψ and $\psi(2S)$. In our calculation, we adopted phenomenological and model-dependent treatment, i.e., the Breit-Wigner ansatz to model the corresponding contribution. In the experiment, these two regions are generally truncated. The CP asymmetry angular coefficients, A_i, are shown to

TABLE V. Theoretical predictions of the $B_c \to D_s^*$ transition form factors at the end point $q^2 = 0$ using different approaches.

	$V^{B_c\to D_s^*}(0)$	$A_0^{B_c\to D_s^*}(0)$	$A_1^{B_c\to D_s^*}(0)$	$A_2^{B_c\to D_s^*}(0)$	$T_1^{B_c\to D_s^*}(0)$	$T_2^{B_c\to D_s^*}(0)$	$T_3^{B_c\to D_s^*}(0)$
This work	0.434	0.387	0.274	0.159	0.265	0.265	0.231
Reference [113]	2.02	0.47	0.56	0.65	⋯	⋯	⋯
Reference [205][a]	0.032	0.016	0.015	0.013	⋯	⋯	⋯
Reference [205][b]	$0.29^{+0.02}_{-0.03}$	$0.16^{+0.01}_{-0.01}$	$0.18^{+0.01}_{-0.02}$	$0.20^{+0.02}_{-0.03}$	⋯	⋯	⋯
Reference [128]	$0.23^{+0.04}_{-0.03}$	$0.17^{+0.01}_{-0.01}$	$0.14^{+0.02}_{-0.01}$	$0.12^{+0.02}_{-0.02}$	⋯	⋯	⋯
Reference [154]	$0.25^{+0.00}_{-0.00}$	$0.18^{+0.02}_{-0.03}$	$0.16^{+0.01}_{-0.02}$	$0.15^{+0.01}_{-0.01}$	⋯	⋯	⋯
Reference [112]	0.336	0.164	0.118	⋯	0.214	0.214	⋯
Reference [112]	0.262	0.139	0.144	⋯	0.167	0.167	⋯
Reference [114]	0.54 ± 0.018	0.30 ± 0.017	0.36 ± 0.013	⋯	0.31 ± 0.017	0.33 ± 0.016	0.29 ± 0.034
Reference [111]	0.33 ± 0.06	0.21 ± 0.04	0.23 ± 0.04	0.25 ± 0.05	0.28 ± 0.06	0.28 ± 0.06	0.27 ± 0.06

[a]These results, listed in the fourth row, are obtained by using the universe parameter $\omega = 0.40$ GeV.

[b]These results, listed in the fifth row, are obtained by using different parameters, i.e., $\omega = 0.96^{+0.08}_{-0.07}$ GeV for the B_c meson and $\omega = 0.51$ GeV for the D_s^* meson.

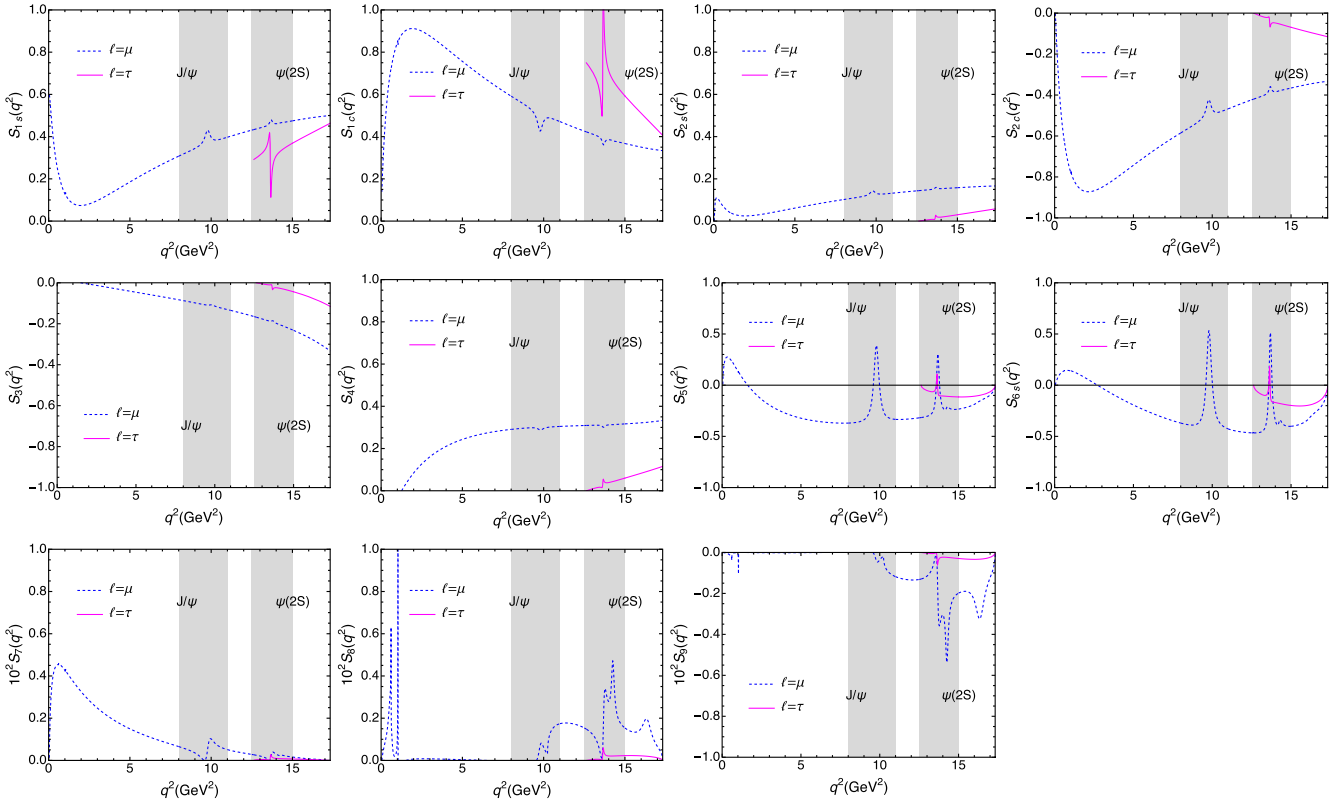

FIG. 5. The q^2 dependence of normalized CP-averaged angular coefficients S_i, where the blue dashed and magenta solid curves are our results for the μ and τ modes, respectively.

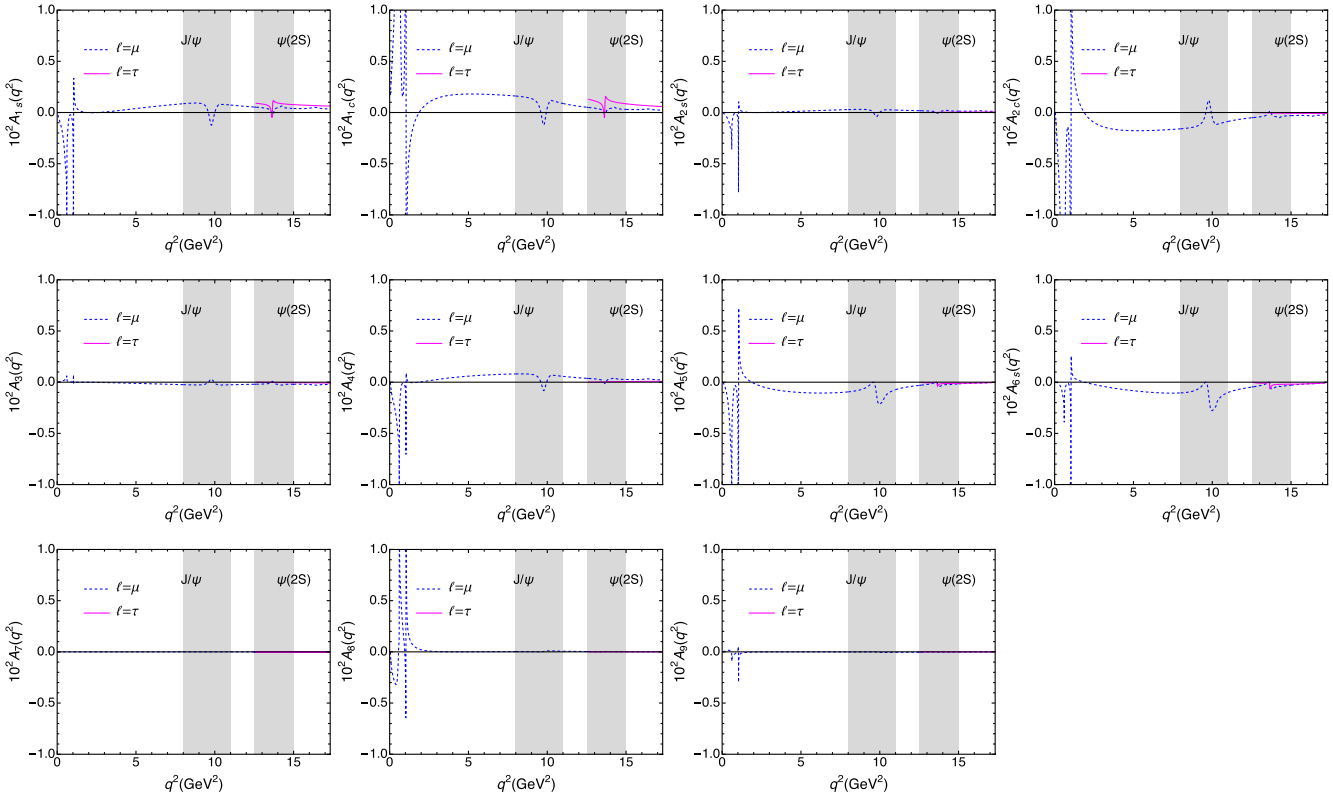

FIG. 6. The q^2 dependence of normalized CP asymmetry angular coefficients A_i, where the blue dashed and magenta solid curves are our results for the μ and τ modes, respectively.

TABLE VI. Our results of the branching fractions of $B_c \to D_s^*(\to D_s\pi)\ell^+\ell^-$ ($\ell = e, \mu, \tau$) (in units of 10^{-8}) in different q^2 bins.

q^2 bins (GeV^2)	$\mathcal{B}(\ell = e)$	$\mathcal{B}(\ell = \mu)$	$\mathcal{B}(\ell = \tau)$
[1.1, 6.0]	0.624	0.622	
		$R^{e\mu} = 1.00$	
[6.0, 8.0]	0.356	0.355	
		$R^{e\mu} = 1.00$	
[11.0, 12.5]	0.283	0.283	
		$R^{e\mu} = 1.00$	
[15.0, 17.0]	0.256	0.256	0.098
		$R^{e\mu} = 1.00, R^{\tau\mu} = 0.384$	

be very small in the SM, due to the direct CP violation being proportional to the $\mathrm{Im}[V_{ub}V_{us}^*/V_{tb}V_{ts}^*]$, which is around 10^{-2}. This character is very clear in Fig. 6. Also, the $S_{7,8,9}$ are also very small compared to the other angular coefficients S_i. These angular coefficients are important physical observables to reveal the underlying decay mechanism, and can be checked by future measurements at LHCb.

We further evaluate the CP-averaged differential branching fractions by using Eqs. (2.21) and (2.22). The q^2 dependence of the differential branching fractions are shown in Fig. 7, where the red, blue and magenta curves represent the e, μ, and τ modes, respectively. The gray areas also denote the charm loop contributions from the charmonium states J/ψ and $\psi(2S)$. In Table VI, we present our result of the branching fractions and their ratios in different q^2 bins. In the four q^2 intervals, i.e., [1.1, 6.0], [6.0, 8.0], [11.0, 12.5], and [15.0, 17.0] GeV^2, the branching fractions of the electron and muon modes can reach up to 10^{-8}, and the ratio $R^{e\mu} = 1$, which is consistent with the SM prediction and reflects the LFU. In the high q^2 region, that is [15.0, 17.0] GeV^2, the branching fraction of the tau mode is on the order of magnitude of 10^{-9}. We also obtain the ratio $R^{\tau\mu} = 0.384$. In the region of $1.1 < q^2 < 6.0$ GeV^2, we have the branching fractions as

$$\mathcal{B}(B_c \to D_s^*(\to D_s\pi)e^+e^-)_{1.1<q^2<6.0\ \mathrm{GeV}^2} = 0.624 \times 10^{-8},$$
$$\mathcal{B}(B_c \to D_s^*(\to D_s\pi)\mu^+\mu^-)_{1.1<q^2<6.0\ \mathrm{GeV}^2} = 0.622 \times 10^{-8}.$$

In addition, combined with the branching fraction $\mathcal{B}(D_s^* \to D_s\pi) = 5\%$, we have

$$\mathcal{B}(B_c \to D_s^* e^+e^-)_{1.1<q^2<6.0\ \mathrm{GeV}^2} = 1.25 \times 10^{-7},$$
$$\mathcal{B}(B_c \to D_s^* \mu^+\mu^-)_{1.1<q^2<6.0\ \mathrm{GeV}^2} = 1.24 \times 10^{-7},$$

which may well be tested by the ongoing LHCb experiment.

We also investigate the physical observables, i.e., the lepton forward-backward asymmetry parameter A_{FB} and the longitudinal (transverse) polarization fractions $F_L(F_T)$. The q^2 dependence of these observables is presented in Figs. 8 and 9, respectively. Their averaged values in different q^2 bins, defined by

$$\langle A\rangle|_{q^2_{\min}}^{q^2_{\max}} = \frac{\int_{q^2_{\min}}^{q^2_{\max}} A[q^2]\left(\frac{d\Gamma}{dq^2} + \frac{d\bar{\Gamma}}{dq^2}\right)dq^2}{\int_{q^2_{\min}}^{q^2_{\max}}\left(\frac{d\Gamma}{dq^2} + \frac{d\bar{\Gamma}}{dq^2}\right)dq^2}, \tag{4.3}$$

where $A = (A_{\mathrm{FB}}, F_L, F_T)$, are shown in Table VII.

In addition, we present our results for the q^2 dependent clean angular observables $P_{1,2,3}$ and $P'_{4,5,6,8}$ in Fig. 10. In Ref. [23], the LHCb collaboration reported the measurement of the form-factor-independent observables $P'_{4,5,6,8}$ of the $B^0 \to K^{*0}\mu^+\mu^-$ decay. In particular, in the interval of $4.30 < q^2 < 8.68$ GeV^2, the observable P'_5 shows 3.7σ discrepancy with the SM prediction [24]. After integration over the energy region $1.0 < q^2 < 6.0$ GeV^2, the discrepancy is determined to be 2.5σ. So we want to investigate these clean angular observables in the rare semileptonic decay of bottom-charmed meson. In order to exclude the charmonium contributions and make it easy to check experimentally, we also present the averaged values of these observables in different q^2 intervals in Table VIII. The averaged value in a q^2 bin is defined by Eq. (4.3).

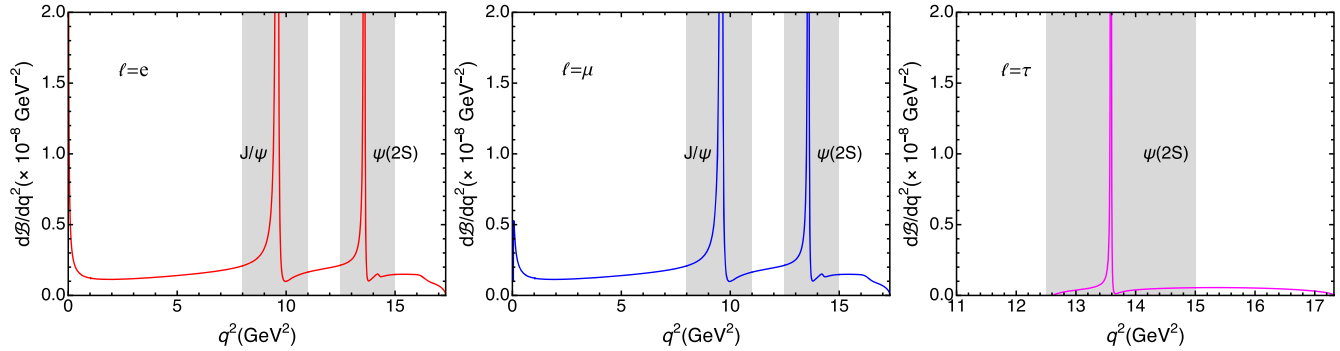

FIG. 7. The q^2 dependence of differential branching fractions $\mathcal{B}(B_c \to D_s^*(\to D_s\pi)\ell^+\ell^-)$ [$\ell = e$ (left panel), μ (center panel), and τ (right panel)], where the red, blue, and magenta curves are our results for the e, μ, and τ modes, respectively.

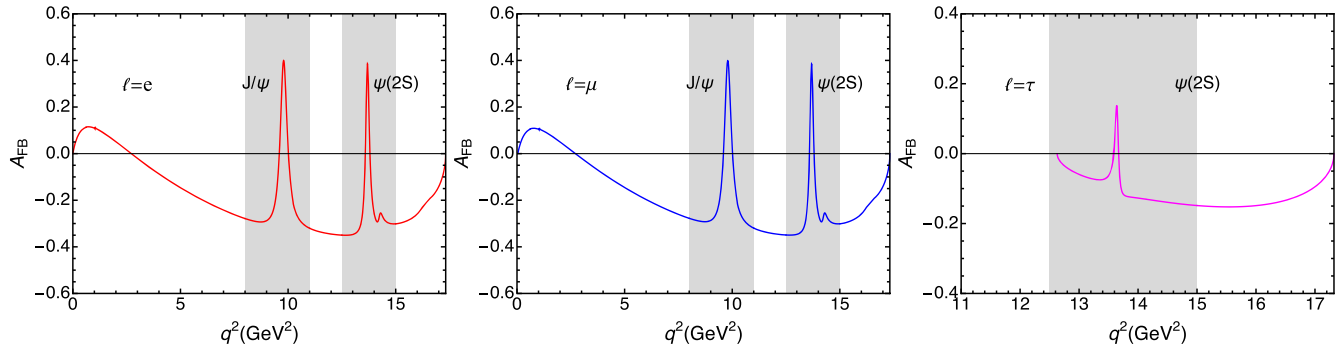

FIG. 8. The q^2 dependence of lepton forward-backward asymmetry parameter $A_{\rm FB}$ in $B_c \to D_s^*(\to D_s\pi)\ell^+\ell^-$ [$\ell = e$ (left panel), μ (center panel), and τ (right panel)] processes, where the red, the blue, and the magenta curves are our results from the e, μ, and τ modes, respectively.

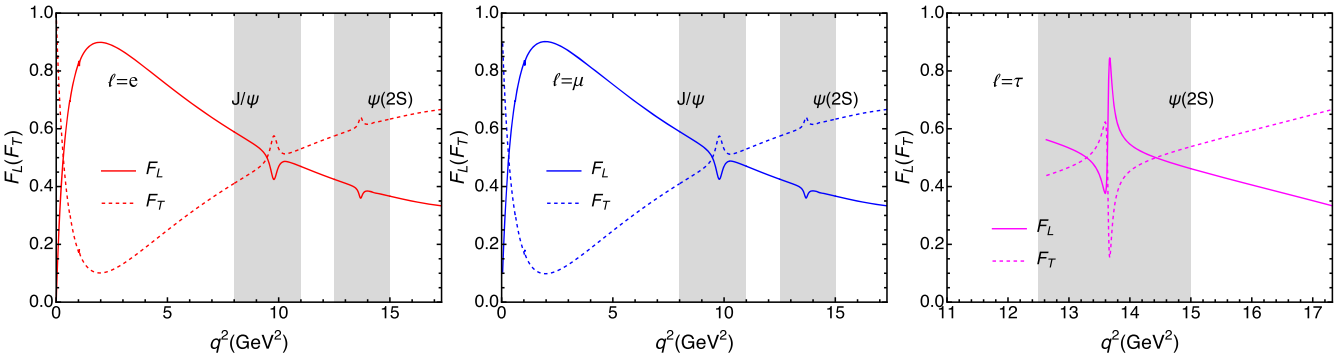

FIG. 9. The q^2 dependence of D_s^* longitudinal (transverse) polarization fractions $F_L(F_T)$ in $B_c \to D_s^*(\to D_s\pi)\ell^+\ell^-$ [$\ell = e$ (left panel), μ (center panel), and τ (right panel)] processes, where the red, the blue, and the magenta curves are our results from the e, μ, and τ modes, respectively, and the solid and dashed curves represent the F_L and F_T, respectively.

TABLE VII. The averaged forward-backward asymmetry $\langle A_{\rm FB}\rangle$ and the longitudinal (transverse) polarization fractions $\langle F_L\rangle(\langle F_T\rangle)$ in different q^2 bins.

q^2 bins (GeV^2)	$\langle A_{\rm FB}(\ell=e)\rangle$	$\langle A_{\rm FB}(\ell=\mu)\rangle$	$\langle A_{\rm FB}(\ell=\tau)\rangle$
[1.1, 6.0]	−0.061	−0.061	
[6.0, 8.0]	−0.243	−0.242	
[11.0, 12.5]	−0.340	−0.339	
[15.0, 17.0]	−0.254	−0.254	−0.143
q^2 bins (GeV^2)	$\langle F_L(\ell=e)\rangle$	$\langle F_L(\ell=\mu)\rangle$	$\langle F_L(\ell=\tau)\rangle$
[1.1, 6.0]	0.815	0.817	
[6.0, 8.0]	0.637	0.638	
[11.0, 12.5]	0.446	0.446	
[15.0, 17.0]	0.352	0.352	0.410
q^2 bins (GeV^2)	$\langle F_T(\ell=e)\rangle$	$\langle F_T(\ell=\mu)\rangle$	$\langle F_T(\ell=\tau)\rangle$
[1.1, 6.0]	0.185	0.183	
[6.0, 8.0]	0.363	0.362	
[11.0, 12.5]	0.554	0.554	
[15.0, 17.0]	0.648	0.648	0.590

In general, this quasi-four-body decay provides a set of physical observables to study the corresponding weak interaction, and in particular the ratios of the branching fractions $R^{e\mu}$ and $R^{\tau\mu}$, as well as the clean angular coefficients P_i and P'_j, can be helpful to search for the NP effects beyond the SM. We call for the ongoing LHCb experiment to search for this process and to measure the corresponding physical observables.

V. SUMMARY

In this work, we have studied the $B_c \to D_s^*$ transition form factors deduced by the (axial) vector and (pseudo) tensor currents, and, in the future, investigate the angular distributions of the quasi-four-body processes $B_c \to D_s^*(\to D_s\pi)\ell^+\ell^-$ ($\ell = e$, μ, τ).

To describe the weak process, the relevant seven independent form factors are calculated by utilizing the covariant LFQM approach. The concerned meson wave functions are adopted as the numerical wave functions, which are extracted from the solution of the modified GI model. This treatment avoids the β dependence and thus reduces the corresponding uncertainty. Our results of form

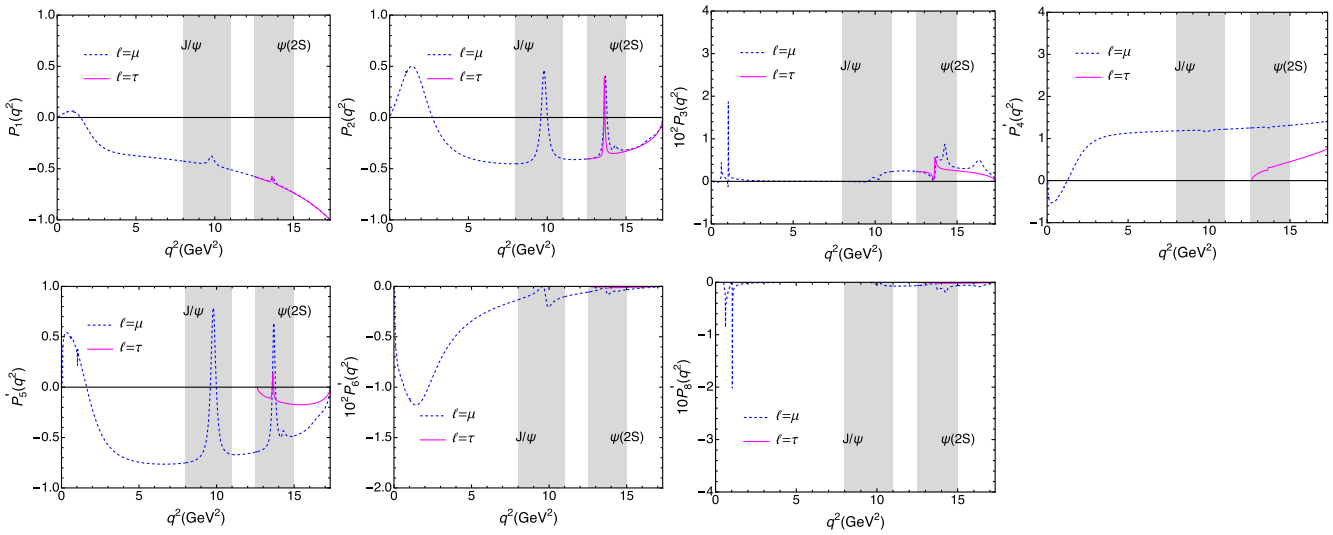

FIG. 10. The q^2 dependence of the clean angular observables $P_{1,2,3}$ and $P'_{4,5,6,8}$, where the blue dashed and magenta solid curves represent our results for the μ and τ modes, respectively.

factors are compared with other approaches. In particular, for the (pseudo)tensor currents deduced form factors $T_{1,2,3}(q^2=0)$, our results agree with the pQCD prediction. More theoretical works, especially the LQCD and QCD sum rule (or light-cone sum rule) calculation, are highly appreciated to test our result and to refine the corresponding topic.

With the obtained form factors, the rare semileptonic decays $B_c \to D_s^*(\to D_s\pi)\ell^+\ell^-$ are studied. Not only the branching fractions, the lepton-side forward-backward asymmetry parameter $A_{\rm FB}$, and the longitudinal and transverse polarization fractions F_L and F_T, but also the angular coefficients S_i and A_i are investigated. Numerically, the concerned cascade decays with e or μ final states are around

TABLE VIII. The averaged values of the clean angular observables $P_{1,2,3}$ and $P'_{4,5,6,8}$ in different q^2 bins.

q^2 bins (GeV^2)	$\langle P_1(\ell=e)\rangle$	$\langle P_1(\ell=\mu)\rangle$	$\langle P_1(\ell=\tau)\rangle$	q^2 bins (GeV^2)	$\langle P_4'(\ell=e)\rangle$	$\langle P_4'(\ell=\mu)\rangle$	$\langle P_4'(\ell=\tau)\rangle$
[1.1, 6.0]	−0.281	−0.281		[1.1, 6.0]	0.908	0.898	
[6.0, 8.0]	−0.408	−0.408		[6.0, 8.0]	1.177	1.169	
[11.0, 12.5]	−0.543	−0.543		[11.0, 12.5]	1.240	1.236	
[15.0, 17.0]	−0.822	−0.822	−0.826	[15.0, 17.0]	1.350	1.347	0.561

q^2 bins (GeV^2)	$\langle P_2(\ell=e)\rangle$	$\langle P_2(\ell=\mu)\rangle$	$\langle P_2(\ell=\tau)\rangle$	q^2 bins (GeV^2)	$\langle P_5'(\ell=e)\rangle$	$\langle P_5'(\ell=\mu)\rangle$	$\langle P_5'(\ell=\tau)\rangle$
[1.1, 6.0]	−0.125	−0.125		[1.1, 6.0]	−0.540	−0.534	
[6.0, 8.0]	−0.446	−0.446		[6.0, 8.0]	−0.766	−0.761	
[11.0, 12.5]	−0.409	−0.409		[11.0, 12.5]	−0.664	−0.662	
[15.0, 17.0]	−0.262	−0.262	−0.269	[15.0, 17.0]	−0.390	−0.390	−0.163

q^2 bins (GeV^2)	$10^3\langle P_3(\ell=e)\rangle$	$10^3\langle P_3(\ell=\mu)\rangle$	$10^3\langle P_3(\ell=\tau)\rangle$	q^2 bins (GeV^2)	$10^3\langle P_6'(\ell=e)\rangle$	$10^3\langle P_6'(\ell=\mu)\rangle$	$10^3\langle P_6'(\ell=\tau)\rangle$
[1.1, 6.0]	0.184	0.184		[1.1, 6.0]	−6.440	−6.320	
[6.0, 8.0]	0.007	0.007		[6.0, 8.0]	−1.868	−1.856	
[11.0, 12.5]	2.421	2.421		[11.0, 12.5]	−0.771	−0.769	
[15.0, 17.0]	3.442	3.442	2.008	[15.0, 17.0]	−0.188	−0.188	−0.070

q^2 bins (GeV^2)	$10^3\langle P_8'(\ell=e)\rangle$	$10^3\langle P_8'(\ell=\mu)\rangle$	$10^3\langle P_8'(\ell=\tau)\rangle$
[1.1, 6.0]	−1.196	−1.164	
[6.0, 8.0]	−0.029	−0.029	
[11.0, 12.5]	−7.054	−7.030	
[15.0, 17.0]	−6.147	−6.137	−1.467

10^{-8}, which need to be tested by other approaches and ongoing experiments. Moreover, the $A_{\rm FB}$ and $F_{L(T)}$ are important physical observables, and they are also feasible observables in the future LHCb experiment, so we look forward to the experimental results. In addition, the ratios of the branching fractions are also calculated to validate whether or not the LFU violated. Furthermore, the clean coefficient observables P_i and P_j' are presented, which reduce the uncertainty from the form factors and can be a possible signal to search for the NP effects. Since these observations are largely free of form factor uncertainties in the large-recoiled limit, and are feasible to measure experimentally, we strongly encourage our experimental colleagues to measure them.

Overall, in this work we have systematically studied the angular distribution of $B_c \to D_s^*(\to D_s\pi)\ell^+\ell^-$ ($\ell = e, \mu, \tau$) with the form factors obtained by the covariant LFQM. We live in the hope that with the completion of the LHCb experiment prepared for the run 3 and run 4 of the LHC and the improvement of the experimental capabilities, this rare semileptonic process can be discovered and we expect that the predicted physical observables can be tested.

ACKNOWLEDGMENTS

This work is supported by the China National Funds for Distinguished Young Scientists under Grant No. 11825503, the National Key Research and Development Program of China under Contract No. 2020YFA0406400, the 111 Project under Grant No. B20063, the National Natural Science Foundation of China under Grants No. 12247101 and No. 12335001, the Fundamental Research Funds for the Central Universities.

APPENDIX: THE WEAK TRANSITION MATRIX ELEMENTS DEDUCED BY AXIAL-VECTOR AND (PSEUDO)TENSOR CURRENTS

In this appendix, we present the concerned expressions of the weak transition matrix elements deduced by axial-vector current, and (pseudo)tensor currents. The expression of the axial-vector current matrix element is

$$\begin{aligned}
S^A_{\mu\nu} &= \mathrm{Tr}\left[\left(\gamma_\nu - \frac{(p_1''-p_2)_\nu}{W_V''}\right)(\not{p}_1'' + m_1'')\gamma_\mu\gamma_5(\not{p}_1' + m_1')\gamma_5(-\not{p}_2 + m_2)\right] \\
&= -2g_{\mu\nu}\Big[m_2(q^2 - N_1' - N_1'' - m_1'^2 - m_1''^2) - m_1'(M''^2 - N_1'' - N_2 - m_1''^2 - m_2^2) \\
&\quad - m_1''(M'^2 - N_1' - N_2 - m_1'^2 - m_2^2) - 2m_1'm_1''m_2\Big] - 8p'_{1\mu}p'_{1\nu}(m_2 - m_1') \\
&\quad + 2m_1'(P_\mu q_\nu + P_\nu q_\mu + 2q_\mu q_\nu) - 2p'_{1\mu}P_\nu(m_1' - m_1'') - 2p'_{1\nu}P_\mu(m_1' + m_1'') \\
&\quad - 2p'_{1\mu}q_\nu(3m_1' - m_1'' - 2m_2) - 2p'_{1\nu}q_\mu(3m_1' + m_1'' - 2m_2) \\
&\quad - \frac{1}{2W_V''}\Big[2p'_{1\mu}(M'^2 + M''^2 - q^2 - 2N_2 + 2(m_1' - m_2)(m_1'' + m_2)) \\
&\quad + q_\mu(q^2 - 2M'^2 + N_1' - N_1'' + 2N_2 - (m_1 + m_1'')^2 + 2(m_1' - m_2)^2) \\
&\quad + P_\mu(q^2 - N_1' - N_1'' - (m_1' + m_1'')^2)\Big](4p'_{1\nu} - 3q_\nu - P_\nu),
\end{aligned} \tag{A1}$$

and the expression of the (pseudo)tensor current matrix element is

$$S^{T+T5}_{\mu\nu} = \mathrm{Tr}\left[\left(\gamma_\nu - \frac{(p_1''-p_2)_\nu}{W_V''}\right)(\not{p}_1'' + m_1'')i\sigma_{\mu\delta}(1+\gamma_5)q^\delta(\not{p}_1' + m_1')\gamma_5(-\not{p}_2 + m_2)\right]. \tag{A2}$$

By using the identity $2\sigma_{\mu\delta}\gamma_5 = -i\epsilon_{\mu\delta\alpha\beta}\sigma^{\alpha\beta}$, the matrix element $S^{T+T5}_{\mu\nu}$ can be decomposed into

$$S^{T+T5}_{\mu\nu} = iq^\delta S_{\mu\nu\delta} + \frac{1}{2}\epsilon_{\mu\delta\alpha\beta}q^\delta S_\nu^{\alpha\beta}, \tag{A3}$$

where $iq^\delta S_{\mu\nu\delta}$ and $\frac{1}{2}\epsilon_{\mu\delta\alpha\beta}q^\delta S_\nu^{\alpha\beta}$ are expressed as

$$
\begin{aligned}
iq^{\delta}S_{\mu\nu\delta} &= \mathrm{Tr}\left[\left(\gamma_{\nu}-\frac{(p_1''-p_2)_{\nu}}{W_V''}\right)(\not{p}_1''+m_1'')i\sigma_{\mu\delta}q^{\delta}(\not{p}_1'+m_1')\gamma_5(-\not{p}_2+m_2)\right] \\
&= i\epsilon_{\mu\nu\alpha\beta}P^{\alpha}p_1^{\beta}(m_1'^2-m_1''^2+N_1'-N_1'')-\frac{i}{2}\epsilon_{\mu\nu\alpha\beta}P^{\alpha}q^{\beta}(m_1'^2+4m_1'm_1''-m_1''^2+N_1'-N_1''+q^2) \\
&\quad -i\epsilon_{\mu\nu\alpha\beta}p_1^{\alpha}q^{\beta}(M'^2-m_1'^2+4m_2(m_1'+m_1'')-4m_1'm_1''-m_1''^2-2m_2^2+M''^2-N_1'-N_1''-2N_2-q^2) \\
&\quad +i\epsilon_{\mu\alpha\beta\gamma}P^{\alpha}p_1^{\beta}q^{\gamma}P_{\nu}\left(\frac{m_1'+m_1''}{W_V''}\right)+i\epsilon_{\mu\alpha\beta\gamma}P^{\alpha}p_1^{\beta}q^{\gamma}p_{1\nu}\left(2-\frac{4(m_1'+m_1'')}{W_V''}\right)+i\epsilon_{\mu\alpha\beta\gamma}P^{\alpha}p_1^{\beta}q^{\gamma}q_{\nu}\left(\frac{3(m_1'+m_1'')}{W_V''}-1\right) \\
&\quad -i\epsilon_{\nu\alpha\beta\gamma}P^{\alpha}p_1^{\beta}q^{\gamma}q_{\mu}+2i\epsilon_{\nu\alpha\beta\gamma}P^{\alpha}p_1^{\beta}q^{\gamma}p_{1\mu}, \qquad \text{(A4)}
\end{aligned}
$$

$$
\begin{aligned}
\frac{1}{2}\epsilon_{\mu\delta\alpha\beta}q^{\delta}S_{\nu}^{\alpha\beta} &= \mathrm{Tr}\left[\left(\gamma_{\nu}-\frac{(p_1''-p_2)_{\nu}}{W_V''}\right)(\not{p}_1''+m_1'')\frac{1}{2}\sigma^{\alpha\beta}\epsilon_{\mu\delta\alpha\beta}q^{\delta}(\not{p}_1'+m_1')\gamma_5(-\not{p}_2+m_2)\right] \\
&= -2ig_{\mu\nu}\{M'^2[m_1''(m_1'-m_1'')-N_1'']+m_1'^3(m_2-m_1'')+m_1'^2(m_2(m_1''-m_2)+M''^2-N_2) \\
&\quad +m_1'(m_1''^3-m_1''^2m_2-m_1''(M''^2+N_1'-N_1'')+m_2(N_1'-N_1''-q^2))-m_1''^3m_2+m_1''^2m_2^2 \\
&\quad +m_1''^2N_2+m_1''m_2N_1'-m_1''m_2N_1''+m_1''m_2q^2-m_2^2N_1'+m_2^2N_1''+M''^2N_1'-N_1'N_2+N_1''N_2\} \\
&\quad +iP_{\mu}P_{\nu}\left\{\frac{(m_1'+m_1'')(m_1'^2-m_1''^2+N_1'-N_1'')+q^2(m_1''-m_1')}{2W_V''}\right\} \\
&\quad +iq_{\mu}q_{\nu}\left\{-2M'^2-m_1'^2+2m_1'm_1''-4m_1'm_2+m_1''^2+2m_2^2-N_1'+N_1''+2N_2-q^2\right. \\
&\quad \left.+\frac{3}{2W_V''}\left[2M'^2m_1'-m_1'^3+m_1'^2(m_1''+2m_2)+m_1'(m_1''^2-2M''^2-N_1'+N_1''-q^2)\right.\right. \\
&\quad \left.\left.-(m_1''+2m_2)(m_1''^2-N_1'+N_1''-q^2)\right]\right\} \\
&\quad +ip_{1\mu}p_{1\nu}\left\{-4M'^2+4M''^2-4q^2+\frac{4}{W_V''}\left[(M'^2-M''^2)(m_1'+m_1'')+q^2(-m_1'+m_1''+2m_2)\right]\right\} \\
&\quad +iP_{\mu}p_{1\nu}\left\{2m_1'^2-2m_1''^2+2N_1'-2N_1''+\frac{2}{W_V''}\left[q^2(m_1'-m_1'')-(m_1'+m_1'')(m_1'^2-m_1''^2+N_1'-N_1'')\right]\right\} \\
&\quad +iP_{\nu}p_{1\mu}\left\{2q^2+\frac{1}{W_V''}\left[q^2(m_1'-m_1''-2m_2)-(M'^2-M''^2)(m_1'+m_1'')\right]\right\} \\
&\quad +iP_{\mu}q_{\nu}\left\{-2m_1'^2+2m_1'm_1''-2N_1'+\frac{3}{2W_V''}\left[(m_1'+m_1'')(m_1'^2-m_1''^2+N_1'-N_1'')+q^2(m_1''-m_1')\right]\right\} \\
&\quad +iP_{\nu}q_{\mu}\left\{-m_1'^2+m_1''^2-N_1'+N_1''-q^2+\frac{1}{2W_V''}\left[2M'^2m_1'-m_1'^3+m_1'^2(m_1''+2m_2)\right.\right. \\
&\quad \left.\left.+m_1'(m_1''^2-2M''^2-N_1'+N_1''-q^2)-(m_1''+2m_2)(m_1''^2-N_1'+N_1''-q^2)\right]\right\} \\
&\quad +ip_{1\mu}q_{\nu}\left\{4M'^2-4m_1'm_1''+4m_1'm_2+4m_1''m_2-4m_2^2-4N_2+2q^2\right. \\
&\quad \left.+\frac{3}{W_V''}\left[q^2(m_1'-m_1''-2m_2)-(M'^2-M''^2)(m_1'+m_1'')\right]\right\} \\
&\quad +ip_{1\nu}q_{\mu}\left\{2M'^2+2m_1'^2-2m_1''^2-2M''^2+2N_1'-2N_1''+2q^2-\frac{2}{W_V''}\left[2M'^2m_1'-m_1'^3+m_1'^2(m_1''+2m_2)\right.\right. \\
&\quad \left.\left.+m_1'(m_1''^2-2M''^2-N_1'+N_1''-q^2)-(m_1''+2m_2)(m_1''^2-N_1'+N_1''-q^2)\right]\right\}, \qquad \text{(A5)}
\end{aligned}
$$

respectively.

[1] W. Altmannshofer and D. M. Straub, New physics in $b \to s$ transitions after LHC run 1, Eur. Phys. J. C **75**, 382 (2015).

[2] S. Descotes-Genon, L. Hofer, J. Matias, and J. Virto, Global analysis of $b \to s\ell\ell$ anomalies, J. High Energy Phys. 06 (2016) 092.

[3] N. R. Singh Chundawat, New physics in $B \to K^*\tau^+\tau^-$: A model independent analysis, Phys. Rev. D **107**, 055004 (2023).

[4] T. Skwarnicki (CLEO Collaboration), Update on $b \to s\gamma$ and $b \to s\ell^+\ell^-$ from CLEO, in *Proceedings of 29th International Conference, ICHEP'98, Vancouver, Canada, July 23–29, Vol. 1, 2* (1998).

[5] T. Affolder *et al.* (CDF Collaboration), Search for the flavor-changing neutral current decays $B^+ \to \mu^+\mu^- K^+$ and $B^0 \to \mu^+\mu^- K^{*0}$, Phys. Rev. Lett. **83**, 3378 (1999).

[6] B. Aubert *et al.* (*BABAR* Collaboration), Search for $B^+ \to K^+\ell^+\ell^-$ and $B^0 \to K^{*0}\ell^+\ell^-$, arXiv:hep-ex/0008059.

[7] K. Abe *et al.* (Belle Collaboration), Observation of the decay $B \to K\ell^+\ell^-$, Phys. Rev. Lett. **88**, 021801 (2001).

[8] A. Ishikawa *et al.* (Belle Collaboration), Observation of $B \to K^*\ell^+\ell^-$, Phys. Rev. Lett. **91**, 261601 (2003).

[9] J. T. Wei *et al.* (Belle Collaboration), Measurement of the differential branching fraction and forward-backward asymmetry for $B \to K^{(*)}\ell^+\ell^-$, Phys. Rev. Lett. **103**, 171801 (2009).

[10] S. Wehle *et al.* (Belle Collaboration), Lepton-flavor-dependent angular analysis of $B \to K^*\ell^+\ell^-$, Phys. Rev. Lett. **118**, 111801 (2017).

[11] S. Choudhury *et al.* (BELLE Collaboration), Test of lepton flavor universality and search for lepton flavor violation in $B \to K\ell\ell$ decays, J. High Energy Phys. 03 (2021) 105.

[12] A. Abdesselam *et al.* (Belle Collaboration), Test of lepton-flavor universality in $B \to K^*\ell^+\ell^-$ decays at Belle, Phys. Rev. Lett. **126**, 161801 (2021).

[13] B. Aubert *et al.* (*BABAR* Collaboration), Evidence for the rare decay $B \to K^*\ell^+\ell^-$ and measurement of the $B \to K\ell^+\ell^-$ branching fraction, Phys. Rev. Lett. **91**, 221802 (2003).

[14] B. Aubert *et al.* (*BABAR* Collaboration), Direct CP, lepton flavor and isospin asymmetries in the decays $B \to K^{(*)}\ell^+\ell^-$, Phys. Rev. Lett. **102**, 091803 (2009).

[15] J. P. Lees *et al.* (*BABAR* Collaboration), Measurement of branching fractions and rate asymmetries in the rare decays $B \to K^{(*)}\ell^+\ell^-$, Phys. Rev. D **86**, 032012 (2012).

[16] T. Aaltonen *et al.* (CDF Collaboration), Observation of the baryonic flavor-changing neutral current decay $\Lambda_b \to \Lambda\mu^+\mu^-$, Phys. Rev. Lett. **107**, 201802 (2011).

[17] V. Khachatryan *et al.* (CMS Collaboration), Angular analysis of the decay $B^0 \to K^{*0}\mu^+\mu^-$ from pp collisions at $\sqrt{s} = 8$ TeV, Phys. Lett. B **753**, 424 (2016).

[18] R. Aaij *et al.* (LHCb Collaboration), Differential branching fraction and angular analysis of the $B^+ \to K^+\mu^+\mu^-$ decay, J. High Energy Phys. 02 (2013) 105.

[19] R. Aaij *et al.* (LHCb Collaboration), Test of lepton universality using $B^+ \to K^+\ell^+\ell^-$ decays, Phys. Rev. Lett. **113**, 151601 (2014).

[20] R. Aaij *et al.* (LHCb Collaboration), Measurements of the S-wave fraction in $B^0 \to K^+\pi^-\mu^+\mu^-$ decays and the $B^0 \to K^{*0}(892)\mu^+\mu^-$ differential branching fraction, J. High Energy Phys. 11 (2016) 047; 04 (2017) 142(E).

[21] R. Aaij *et al.* (LHCb Collaboration), Test of lepton universality with $B^0 \to K^{*0}\ell^+\ell^-$ decays, J. High Energy Phys. 08 (2017) 055.

[22] R. Aaij *et al.* (LHCb Collaboration), Test of lepton universality in beauty-quark decays, Nat. Phys. **18**, 277 (2022).

[23] R. Aaij *et al.* (LHCb Collaboration), Measurement of form-factor-independent observables in the decay $B^0 \to K^{*0}\mu^+\mu^-$, Phys. Rev. Lett. **111**, 191801 (2013).

[24] U. Egede, T. Hurth, J. Matias, M. Ramon, and W. Reece, New observables in the decay mode $\bar{B}_d \to \bar{K}^{*0}\ell^+\ell^-$, J. High Energy Phys. 11 (2008) 032.

[25] M. Bordone, G. Isidori, and A. Pattori, On the standard model predictions for R_K and R_{K^*}, Eur. Phys. J. C **76**, 440 (2016).

[26] D. Acosta *et al.* (CDF Collaboration), Search for the decay $B_s \to \mu^+\mu^-\phi$ in $p\bar{p}$ collisions at $\sqrt{s} = 1.8$-TeV, Phys. Rev. D **65**, 111101 (2002).

[27] T. Aaltonen *et al.* (CDF Collaboration), Search for the rare decays $B^+ \to \mu^+\mu^- K^+$, $B^0 \to \mu^+\mu^- K^{*0}(892)$, and $B_s^0 \to \mu^+\mu^-\phi$ at CDF, Phys. Rev. D **79**, 011104 (2009).

[28] V. M. Abazov *et al.* (D0 Collaboration), Search for the rare decay $B_s^0 \to \phi\mu^+\mu^-$ with the D0 detector, Phys. Rev. D **74**, 031107 (2006).

[29] T. Aaltonen *et al.* (CDF Collaboration), Measurement of the forward-backward asymmetry in the $B \to K^{(*)}\mu^+\mu^-$ decay and first observation of the $B_s^0 \to \phi\mu^+\mu^-$ decay, Phys. Rev. Lett. **106**, 161801 (2011).

[30] R. Aaij *et al.* (LHCb Collaboration), Differential branching fraction and angular analysis of the decay $B_s^0 \to \phi\mu^+\mu^-$, J. High Energy Phys. 07 (2013) 084.

[31] R. Aaij *et al.* (LHCb Collaboration), Angular analysis and differential branching fraction of the decay $B_s^0 \to \phi\mu^+\mu^-$, J. High Energy Phys. 09 (2015) 179.

[32] R. Aaij *et al.* (LHCb Collaboration), Branching fraction measurements of the rare $B_s^0 \to \phi\mu^+\mu^-$ and $B_s^0 \to f_2'(1525)\mu^+\mu^-$ decays, Phys. Rev. Lett. **127**, 151801 (2021).

[33] T. V. Dong *et al.* (Belle Collaboration), Search for the decay $B_0 \to K^{*0}\tau^+\tau^-$ at the Belle experiment, Phys. Rev. D **108**, L011102 (2023).

[34] C. Bouchard *et al.* (HPQCD Collaboration), Rare decay $B \to K\ell^+\ell^-$ form factors from lattice QCD, Phys. Rev. D **88**, 054509 (2013); **88**, 079901(E) (2013).

[35] R. R. Horgan, Z. Liu, S. Meinel, and M. Wingate, Lattice QCD calculation of form factors describing the rare decays $B \to K^*\ell^+\ell^-$ and $B_s \to \phi\ell^+\ell^-$, Phys. Rev. D **89**, 094501 (2014).

[36] J. A. Bailey, A. Bazavov, C. Bernard, C. M. Bouchard, C. DeTar, D. Du, A. X. El-Khadra, J. Foley, E. D. Freeland, E. Gámiz *et al.*, $B \to K\ell^+\ell^-$ decay form factors from three-flavor lattice QCD, Phys. Rev. D **93**, 025026 (2016).

[37] P. Ball and R. Zwicky, $B_{d,s} \to \rho, \omega, K^*, \phi$ decay form-factors from light-cone sum rules revisited, Phys. Rev. D **71**, 014029 (2005).

[38] P. Ball and R. Zwicky, New results on $B \to \pi, K, \eta$ decay form factors from light-cone sum rules, Phys. Rev. D **71**, 014015 (2005).

[39] Y. L. Wu, M. Zhong, and Y. B. Zuo, $B_s, D_s \to \pi, K, \eta, \rho, K^*, \omega, \phi$ transition form factors and decay rates

with extraction of the CKM parameters $|V_{ub}|$, $|V_{cs}|$, $|V_{cd}|$, Int. J. Mod. Phys. A **21**, 6125 (2006).
[40] M. Bartsch, M. Beylich, G. Buchalla, and D. N. Gao, Precision flavour physics with $B \to K\nu\bar{\nu}$ and $B \to K\ell^+\ell^-$, J. High Energy Phys. 11 (2009) 011.
[41] A. Bharucha, D. M. Straub, and R. Zwicky, $B \to V\ell^+\ell^-$ in the standard model from light-cone sum rules, J. High Energy Phys. 08 (2016) 098.
[42] W. Cheng, X. G. Wu, and H. B. Fu, Reconsideration of the $B \to K^*$ transition form factors within the QCD light-cone sum rules, Phys. Rev. D **95**, 094023 (2017).
[43] J. Gao, C. D. Lü, Y. L. Shen, Y. M. Wang, and Y. B. Wei, Precision calculations of $B \to V$ form factors from soft-collinear effective theory sum rules on the light-cone, Phys. Rev. D **101**, 074035 (2020).
[44] Y. M. Wang and Y. L. Shen, QCD corrections to $B \to \pi$ form factors from light-cone sum rules, Nucl. Phys. **B898**, 563 (2015).
[45] Y. M. Wang, Y. B. Wei, Y. L. Shen, and C. D. Lü, Perturbative corrections to $B \to D$ form factors in QCD, J. High Energy Phys. 06 (2017) 062.
[46] C. D. Lü, Y. L. Shen, Y. M. Wang, and Y. B. Wei, QCD calculations of $B \to \pi, K$ form factors with higher-twist corrections, J. High Energy Phys. 01 (2019) 024.
[47] J. Gao, T. Huber, Y. Ji, C. Wang, Y. M. Wang, and Y. B. Wei, $B \to D\ell\nu_\ell$ form factors beyond leading power and extraction of $|V_{cb}|$ and R_D, J. High Energy Phys. 05 (2022) 024.
[48] B. Y. Cui, Y. K. Huang, Y. L. Shen, C. Wang, and Y. M. Wang, Precision calculations of $B_{d,s} \to \pi, K$ decay form factors in soft-collinear effective theory, J. High Energy Phys. 03 (2023) 140.
[49] B. Y. Cui, Y. K. Huang, Y. M. Wang, and X. C. Zhao, Shedding new light on $\mathcal{R}(D_{(s)}^{(*)})$ and $|V_{cb}|$ from semileptonic $\bar{B}_{(s)} \to D_{(s)}^{(*)}\ell\bar{\nu}_\ell$ decays, Phys. Rev. D **108**, L071504 (2023).
[50] C. Bobeth, G. Hiller, and G. Piranishvili, *CP* asymmetries in bar $B \to \bar{K}^*(\to \bar{K}\pi)\bar{\ell}\ell$ and untagged $\bar{B}_s$, $B_s \to \phi(\to K^+K^-)\bar{\ell}\ell$ decays at NLO, J. High Energy Phys. 07 (2008) 106.
[51] R. H. Li, C. D. Lü, and W. Wang, Transition form factors of B decays into p-wave axial-vector mesons in the perturbative QCD approach, Phys. Rev. D **79**, 034014 (2009).
[52] W. Wang, R. H. Li, and C. D. Lü, Radiative charmless $B_s \to V\gamma$ and $B_s \to A\gamma$ decays in pQCD approach, arXiv:0711.0432.
[53] R. H. Li, C. D. Lü, and W. Wang, Branching ratios, forward-backward asymmetry and angular distributions of $B \to K_1\ell^+\ell^-$ decays, Phys. Rev. D **79**, 094024 (2009).
[54] W. F. Wang and Z. J. Xiao, The semileptonic decays $B/B_s \to (\pi, K)(\ell^+\ell^-, \ell\nu, \nu\bar{\nu})$ in the perturbative QCD approach beyond the leading-order, Phys. Rev. D **86**, 114025 (2012).
[55] W. F. Wang, Y. Y. Fan, M. Liu, and Z. J. Xiao, Semileptonic decays $B/B_s \to (\eta, \eta', G)(\ell^+\ell^-, \ell\bar{\nu}, \nu\bar{\nu})$ in the perturbative QCD approach beyond the leading order, Phys. Rev. D **87**, 097501 (2013).
[56] Z. J. Xiao and X. Liu, The two-body hadronic decays of B_c meson in the perturbative QCD approach: A short review, Chin. Sci. Bull. **59**, 3748 (2014).
[57] S. P. Jin, X. Q. Hu, and Z. J. Xiao, Study of $B_s \to K^{(*)}\ell^+\ell^-$ decays in the PQCD factorization approach with lattice QCD input, Phys. Rev. D **102**, 013001 (2020).
[58] S. P. Jin and Z. J. Xiao, Study of $B_s \to \phi\ell^+\ell^-$ decays in the PQCD factorization approach with lattice QCD input, Adv. High Energy Phys. **2021**, 3840623 (2021).
[59] A. Deandrea and A. D. Polosa, The exclusive $B_s \to \phi\mu^+\mu^-$ process in a constituent quark model, Phys. Rev. D **64**, 074012 (2001).
[60] C. Q. Geng and C. C. Liu, Study of $B_s \to (\eta, \eta', \phi)\ell\overline{\ell}$ decays, J. Phys. G **29**, 1103 (2003).
[61] C. H. Chen, C. Q. Geng, and W. Wang, Z-mediated charge and *CP* asymmetries and FCNCs in $B_{d,s}$ processes, J. High Energy Phys. 11 (2010) 089.
[62] R. H. Li, C. D. Lü, and W. Wang, Branching ratios, forward-backward asymmetries and angular distributions of $B \to K_2^*\ell^+\ell^-$ in the standard model and new physics scenarios, Phys. Rev. D **83**, 034034 (2011).
[63] S. Dubnička, A. Z. Dubničková, A. Issadykov, M. A. Ivanov, A. Liptaj, and S. K. Sakhiyev, Decay $B_s \to \phi\ell^+\ell^-$ in covariant quark model, Phys. Rev. D **93**, 094022 (2016).
[64] N. R. Soni, A. Issadykov, A. N. Gadaria, J. J. Patel, and J. N. Pandya, Rare $b \to d$ decays in covariant confined quark model, Eur. Phys. J. A **58**, 39 (2022).
[65] A. Issadykov, $B_s^0 \to \bar{K}^*(892)^0\ell^+\ell^-$ decay in covariant confined quark model, Phys. Part. Nucl. Lett. **19**, 460 (2022).
[66] C. D. Lü and W. Wang, Analysis of $B \to K_J^*(\to K\pi)\mu^+\mu^-$ in the higher kaon resonance region, Phys. Rev. D **85**, 034014 (2012).
[67] M. Ahmady, S. Keller, M. Thibodeau, and R. Sandapen, Reexamination of the rare decay $B_s \to \phi\mu^+\mu^-$ using holographic light-front QCD, Phys. Rev. D **100**, 113005 (2019).
[68] N. Rajeev, N. Sahoo, and R. Dutta, Angular analysis of $B_s \to f_2'(1525)(\to K^+K^-)\mu^+\mu^-$ decays as a probe to lepton flavor universality violation, Phys. Rev. D **103**, 095007 (2021).
[69] S. P. Li, X. Q. Li, Y. D. Yang, and X. Zhang, $R_{D^{(*)}}, R_{K^{(*)}}$ and neutrino mass in the 2HDM-III with right-handed neutrinos, J. High Energy Phys. 09 (2018) 149.
[70] B. Barman, D. Borah, L. Mukherjee, and S. Nandi, Correlating the anomalous results in $b \to s$ decays with inert Higgs doublet dark matter and muon $(g-2)$, Phys. Rev. D **100**, 115010 (2019).
[71] L. Delle Rose, S. Khalil, S. J. D. King, and S. Moretti, R_K and R_{K^*} in an aligned 2HDM with right-handed neutrinos, Phys. Rev. D **101**, 115009 (2020).
[72] A. Ordell, R. Pasechnik, H. Serôdio, and F. Nottensteiner, Classification of anomaly-free 2HDMs with a gauged $U(1)'$ symmetry, Phys. Rev. D **100**, 115038 (2019).
[73] C. Marzo, L. Marzola, and M. Raidal, Common explanation to the $R_{K^{(*)}}$, $R_{D^{(*)}}$ and ϵ'/ϵ anomalies in a 3HDM + ν_R and connections to neutrino physics, Phys. Rev. D **100**, 055031 (2019).

[74] S. Iguro and Y. Omura, Status of the semileptonic B decays and muon $g-2$ in general 2HDMs with right-handed neutrinos, J. High Energy Phys. 05 (2018) 173.

[75] S. Iguro, Conclusive probe of the charged Higgs solution of P_5' and $R_{D^{(*)}}$ discrepancies, Phys. Rev. D **107**, 095004 (2023).

[76] M. J. Aslam, C. D. Lü, and Y. M. Wang, $B \to K_0^*(1430)\ell^+\ell^-$ decays in supersymmetric theories, Phys. Rev. D **79**, 074007 (2009).

[77] S. Trifinopoulos, B-physics anomalies: The bridge between R-parity violating supersymmetry and flavored dark matter, Phys. Rev. D **100**, 115022 (2019).

[78] A. Shaw, Looking for $B \to X_s\ell^+\ell^-$ in a nonminimal universal extra dimensional model, Phys. Rev. D **99**, 115030 (2019).

[79] W. Altmannshofer, S. Gori, M. Pospelov, and I. Yavin, Quark flavor transitions in $L_\mu - L_\tau$ models, Phys. Rev. D **89**, 095033 (2014).

[80] B. Bhattacharya, A. Datta, D. London, and S. Shivashankara, Simultaneous explanation of the R_K and $R(D^{(*)})$ puzzles, Phys. Lett. B **742**, 370 (2015).

[81] A. Crivellin, G. D'Ambrosio, and J. Heeck, Addressing the LHC flavor anomalies with horizontal gauge symmetries, Phys. Rev. D **91**, 075006 (2015).

[82] A. Celis, J. Fuentes-Martin, M. Jung, and H. Serodio, Family nonuniversal Z' models with protected flavor-changing interactions, Phys. Rev. D **92**, 015007 (2015).

[83] A. Falkowski, M. Nardecchia, and R. Ziegler, Lepton flavor non-universality in B-meson decays from a U(2) flavor model, J. High Energy Phys. 11 (2015) 173.

[84] B. Bhattacharya, A. Datta, J. P. Guévin, D. London, and R. Watanabe, Simultaneous explanation of the R_K and $R_{D^{(*)}}$ puzzles: A model analysis, J. High Energy Phys. 01 (2017) 015.

[85] C. W. Chiang, X. G. He, J. Tandean, and X. B. Yuan, $R_{K^{(*)}}$ and related $b \to s\ell\bar{\ell}$ anomalies in minimal flavor violation framework with Z' boson, Phys. Rev. D **96**, 115022 (2017).

[86] S. F. King, Flavourful Z' models for $R_{K^{(*)}}$, J. High Energy Phys. 08 (2017) 019.

[87] A. Falkowski, S. F. King, E. Perdomo, and M. Pierre, Flavourful Z' portal for vector-like neutrino dark matter and $R_{K^{(*)}}$, J. High Energy Phys. 08 (2018) 061.

[88] B. C. Allanach, J. M. Butterworth, and T. Corbett, Collider constraints on Z' models for neutral current B-anomalies, J. High Energy Phys. 08 (2019) 106.

[89] S. Dwivedi, D. Kumar Ghosh, A. Falkowski, and N. Ghosh, Associated Z' production in the flavorful U(1) scenario for $R_{K^{(*)}}$, Eur. Phys. J. C **80**, 263 (2020).

[90] B. Capdevila, A. Crivellin, C. A. Manzari, and M. Montull, Explaining $b \to s\ell^+\ell^-$ and the Cabibbo angle anomaly with a vector triplet, Phys. Rev. D **103**, 015032 (2021).

[91] J. H. Sheng, The analysis of $b \to s\ell^+\ell^-$ in the family non-universal Z' model, Int. J. Theor. Phys. **60**, 26 (2021).

[92] G. Hiller and M. Schmaltz, R_K and future $b \to s\ell\ell$ physics beyond the standard model opportunities, Phys. Rev. D **90**, 054014 (2014).

[93] B. Gripaios, M. Nardecchia, and S. A. Renner, Composite leptoquarks and anomalies in B-meson decays, J. High Energy Phys. 05 (2015) 006.

[94] I. de Medeiros Varzielas and G. Hiller, Clues for flavor from rare lepton and quark decays, J. High Energy Phys. 06 (2015) 072.

[95] D. Bečirević and O. Sumensari, A leptoquark model to accommodate $R_K^{\rm exp} < R_K^{\rm SM}$ and $R_{K^*}^{\rm exp} < R_{K^*}^{\rm SM}$, J. High Energy Phys. 08 (2017) 104.

[96] L. Di Luzio, A. Greljo, and M. Nardecchia, Gauge leptoquark as the origin of B-physics anomalies, Phys. Rev. D **96**, 115011 (2017).

[97] D. Bečirević, I. Doršner, S. Fajfer, N. Košnik, D. A. Faroughy, and O. Sumensari, Scalar leptoquarks from grand unified theories to accommodate the B-physics anomalies, Phys. Rev. D **98**, 055003 (2018).

[98] A. Angelescu, D. Bečirević, D. A. Faroughy, and O. Sumensari, Closing the window on single leptoquark solutions to the B-physics anomalies, J. High Energy Phys. 10 (2018) 183.

[99] C. Cornella, J. Fuentes-Martin, and G. Isidori, Revisiting the vector leptoquark explanation of the B-physics anomalies, J. High Energy Phys. 07 (2019) 168.

[100] O. Popov, M. A. Schmidt, and G. White, R_2 as a single leptoquark solution to $R_{D^{(*)}}$ and $R_{K^{(*)}}$, Phys. Rev. D **100**, 035028 (2019).

[101] L. Da Rold and F. Lamagna, A vector leptoquark for the B-physics anomalies from a composite GUT, J. High Energy Phys. 12 (2019) 112.

[102] C. Hati, J. Kriewald, J. Orloff, and A. M. Teixeira, A nonunitary interpretation for a single vector leptoquark combined explanation to the B-decay anomalies, J. High Energy Phys. 12 (2019) 006.

[103] A. Datta, J. L. Feng, S. Kamali, and J. Kumar, Resolving the $(g-2)_\mu$ and B anomalies with leptoquarks and a dark Higgs boson, Phys. Rev. D **101**, 035010 (2020).

[104] S. Balaji and M. A. Schmidt, Unified SU(4) theory for the $R_{D^{(*)}}$ and $R_{K^{(*)}}$ anomalies, Phys. Rev. D **101**, 015026 (2020).

[105] A. Crivellin, D. Müller, and F. Saturnino, Flavor phenomenology of the leptoquark singlet-triplet model, J. High Energy Phys. 06 (2020) 020.

[106] S. Saad, Combined explanations of $(g-2)_\mu$, $R_{D^{(*)}}$, $R_{K^{(*)}}$ anomalies in a two-loop radiative neutrino mass model, Phys. Rev. D **102**, 015019 (2020).

[107] K. S. Babu, P. S. B. Dev, S. Jana, and A. Thapa, Unified framework for B-anomalies, muon $g-2$ and neutrino masses, J. High Energy Phys. 03 (2021) 179.

[108] S. Iguro, J. Kawamura, S. Okawa, and Y. Omura, TeV-scale vector leptoquark from Pati-Salam unification with vectorlike families, Phys. Rev. D **104**, 075008 (2021).

[109] R. Aaij *et al.* (LHCb Collaboration), Measurement of the B_c^- meson production fraction and asymmetry in 7 and 13 TeV pp collisions, Phys. Rev. D **100**, 112006 (2019).

[110] R. Aaij *et al.* (LHCb Collaboration), A search for rare $B \to D\mu^+\mu^-$ decays, arXiv:2308.06162.

[111] W. F. Wang, X. Yu, C. D. Lü, and Z. J. Xiao, Semileptonic decays $B_c^+ \to D_{(s)}^{(*)}(\ell^+\nu_\ell, \ell^+\ell^-, \nu\bar{\nu})$ in the perturbative QCD approach, Phys. Rev. D **90**, 094018 (2014).

[112] C. Q. Geng, C. W. Hwang, and C. C. Liu, Study of rare $B_c^+ \to D_{d,s}^{(*)+}\ell\bar{\ell}$ decays, Phys. Rev. D **65**, 094037 (2002).

[113] V. V. Kiselev, Exclusive decays and lifetime of B_c meson in QCD sum rules, arXiv:hep-ph/0211021.

[114] K. Azizi, F. Falahati, V. Bashiry, and S. M. Zebarjad, Analysis of the rare $B_c \to D^*_{(s,d)}\ell^+\ell^-$ decays in QCD, Phys. Rev. D **77**, 114024 (2008).

[115] R. Dutta, Model independent analysis of new physics effects on $B_c \to (D_s, D_s^*)\mu^+\mu^-$ decay observables, Phys. Rev. D **100**, 075025 (2019).

[116] M. K. Mohapatra, N. Rajeev, and R. Dutta, Combined analysis of $B_c \to D_s^{(*)}\mu^+\mu^-$ and $B_c \to D_s^{(*)}\nu\bar{\nu}$ decays within Z' and leptoquark new physics models, Phys. Rev. D **105**, 115022 (2022).

[117] M. Zaki, M. A. Paracha, and F. M. Bhutta, Footprints of new physics in the angular distribution of $B_c \to D_s^*(\to D_s\gamma, (D_s\pi))\ell^+\ell^-$ decays, Nucl. Phys. **B992**, 116236 (2023).

[118] W. Jaus, Semileptonic decays of B and D mesons in the light front formalism, Phys. Rev. D **41**, 3394 (1990).

[119] W. Jaus, Semileptonic, radiative, and pionic decays of B, B^* and D, D^* mesons, Phys. Rev. D **53**, 1349 (1996); **54**, 5904(E) (1996).

[120] H. Y. Cheng, C. Y. Cheung, and C. W. Hwang, Mesonic form factors and the Isgur-Wise function on the light front, Phys. Rev. D **55**, 1559 (1997).

[121] H. Y. Cheng, C. Y. Cheung, C. W. Hwang, and W. M. Zhang, A covariant light front model of heavy mesons within HQET, Phys. Rev. D **57**, 5598 (1998).

[122] W. Jaus, Covariant analysis of the light front quark model, Phys. Rev. D **60**, 054026 (1999).

[123] H. Y. Cheng and C. K. Chua, Covariant light front approach for $B \to K^*\gamma, K_1\gamma, K_2^*\gamma$ decays, Phys. Rev. D **69**, 094007 (2004); **81**, 059901(E) (2010).

[124] H. Y. Cheng, C. K. Chua, and C. W. Hwang, Covariant light front approach for s-wave and p-wave mesons: Its application to decay constants and form factors, Phys. Rev. D **69**, 074025 (2004).

[125] C. K. Chua, Covariant light front approach for s-wave and p-wave mesons, J. Korean Phys. Soc. **45**, S256 (2004).

[126] W. Wang, Y. L. Shen, and C. D. Lü, The study of $B_c \to X(3872)\pi^-(K^-)$ decays in the covariant light-front approach, Eur. Phys. J. C **51**, 841 (2007).

[127] W. Wang and Y. L. Shen, $D_s \to K, K^*, \phi$ form factors in the covariant light-front approach and exclusive D_s decays, Phys. Rev. D **78**, 054002 (2008).

[128] W. Wang, Y. L. Shen, and C. D. Lü, Covariant light-front approach for B_c transition form factors, Phys. Rev. D **79**, 054012 (2009).

[129] Y. L. Shen and Y. M. Wang, J/ψ weak decays in the covariant light-front quark model, Phys. Rev. D **78**, 074012 (2008).

[130] X. X. Wang, W. Wang, and C. D. Lu, B_c to p-wave charmonia transitions in covariant light-front approach, Phys. Rev. D **79**, 114018 (2009).

[131] C. H. Chen, Y. L. Shen, and W. Wang, $|V_{ub}|$ and $B \to \eta^{(\prime)}$ form factors in covariant light front approach, Phys. Lett. B **686**, 118 (2010).

[132] H. Y. Cheng and C. K. Chua, $B \to V, A, T$ tensor form factors in the covariant light-front approach: Implications on radiative B decays, Phys. Rev. D **81**, 114006 (2010); **82**, 059904(E) (2010).

[133] H. M. Choi, Exclusive rare $B_s \to (K, \eta, \eta')\ell^+\ell^-$ decays in the light-front quark model, J. Phys. G **37**, 085005 (2010).

[134] G. Li, F. l. Shao, and W. Wang, $B_s \to D_s(3040)$ form factors and B_s decays into $D_s(3040)$, Phys. Rev. D **82**, 094031 (2010).

[135] H. M. Choi and C. R. Ji, Light-front dynamic analysis of transition form factors in the process of $P \to V\ell\nu_\ell$, Nucl. Phys. **A856**, 95 (2011).

[136] H. W. Ke and X. Q. Li, Vertex functions for d-wave mesons in the light-front approach, Eur. Phys. J. C **71**, 1776 (2011).

[137] R. C. Verma, Decay constants and form factors of s-wave and p-wave mesons in the covariant light-front quark model, J. Phys. G **39**, 025005 (2012).

[138] H. W. Ke, T. Liu, and X. Q. Li, Transitions of $B_c \to \psi(1S, 2S)$ and the modified harmonic oscillator wave function in LFQM, Phys. Rev. D **89**, 017501 (2014).

[139] H. Xu, Q. Huang, H. W. Ke, and X. Liu, Numerical analysis of the production of $D^{(*)}(3000)$, $D_{sJ}(3040)$ and their partners through the semileptonic decays of $B_{(s)}$ mesons in terms of the light front quark model, Phys. Rev. D **90**, 094017 (2014).

[140] Y. J. Shi, W. Wang, and Z. X. Zhao, $B_c \to B_{sJ}$ form factors and B_c decays into B_{sJ} in covariant light-front approach, Eur. Phys. J. C **76**, 555 (2016).

[141] K. Chen, H. W. Ke, X. Liu, and T. Matsuki, Estimating the production rates of D-wave charmed mesons via the semileptonic decays of bottom mesons, Chin. Phys. C **43**, 023106 (2019).

[142] H. Y. Cheng and X. W. Kang, Branching fractions of semileptonic D and D_s decays from the covariant light-front quark model, Eur. Phys. J. C **77**, 587 (2017); **77**, 863 (E) (2017).

[143] X. W. Kang, T. Luo, Y. Zhang, L. Y. Dai, and C. Wang, Semileptonic B and B_s decays involving scalar and axial-vector mesons, Eur. Phys. J. C **78**, 909 (2018).

[144] Q. Chang, X. N. Li, X. Q. Li, F. Su, and Y. D. Yang, Self-consistency and covariance of light-front quark models: Testing via P, V and A meson decay constants, and $P \to P$ weak transition form factors, Phys. Rev. D **98**, 114018 (2018).

[145] Q. Chang, Y. Zhang, and X. Li, Study of $\bar{B}^*_{u,d,s} \to D^*_{u,d,s}V, (V = D^{*-}_{d,s}, K^{*-}, \rho^-)$ weak decays, Chin. Phys. C **43**, 103104 (2019).

[146] Q. Chang, L. T. Wang, and X. N. Li, Form factors of $V' \to V''$ transition within the light-front quark models, J. High Energy Phys. 12 (2019) 102.

[147] Q. Chang, X. N. Li, and L. T. Wang, Revisiting the form factors of $P \to V$ transition within the light-front quark models, Eur. Phys. J. C **79**, 422 (2019).

[148] Q. Chang, X. L. Wang, J. Zhu, and X. N. Li, Study of $b \to c$ induced $\bar{B}^* \to V\ell\bar{\nu}_\ell$ decays, Adv. High Energy Phys. **2020**, 3079670 (2020).

[149] Q. Chang, X. L. Wang, and L. T. Wang, Tensor form factors of $P \to P, S, V$ and A transitions within standard and covariant light-front approaches, Chin. Phys. C **44**, 083105 (2020).

[150] H. M. Choi, Self-consistent light-front quark model analysis of $B \to D\ell\nu_\ell$ transition form factors, Phys. Rev. D **103**, 073004 (2021).

[151] H. M. Choi, Current-component independent transition form factors for semileptonic and rare $D \to \pi K$ decays

in the light-front quark model, Adv. High Energy Phys. **2021**, 4277321 (2021).
[152] L. Chen, Y. W. Ren, L. T. Wang, and Q. Chang, Form factors of $P \to T$ transition within the light-front quark models, Eur. Phys. J. C **82**, 451 (2022).
[153] A. J. Arifi, H. M. Choi, C. R. Ji, and Y. Oh, Independence of current components, polarization vectors, and reference frames in the light-front quark model analysis of meson decay constants, Phys. Rev. D **107**, 053003 (2023).
[154] Z. Q. Zhang, Z. J. Sun, Y. C. Zhao, Y. Y. Yang, and Z. Y. Zhang, Covariant light-front approach for B_c decays into charmonium: Implications on form factors and branching ratios, Eur. Phys. J. C **83**, 477 (2023).
[155] Y. J. Shi and Z. P. Xing, Heavy flavor conserved semileptonic decay of B_s in the covariant light-front approach, arXiv:2307.02767.
[156] A. Hazra, T. M. S., N. Sharma, and R. Dhir, B_c to A transition form factors and semileptonic decays in self-consistent covariant light-front approach, arXiv:2309.03655.
[157] L. Zhang, X. W. Kang, X. H. Guo, L. Y. Dai, T. Luo, and C. Wang, A comprehensive study on the semileptonic decay of heavy flavor mesons, J. High Energy Phys. 02 (2021) 179.
[158] H. W. Ke, X. Q. Li, and Z. T. Wei, Diquarks and $\Lambda_b \to \Lambda_c$ weak decays, Phys. Rev. D **77**, 014020 (2008).
[159] H. W. Ke, X. H. Yuan, X. Q. Li, Z. T. Wei, and Y. X. Zhang, $\Sigma_b \to \Sigma_c$ and $\Omega_b \to \Omega_c$ weak decays in the light-front quark model, Phys. Rev. D **86**, 114005 (2012).
[160] H. W. Ke, N. Hao, and X. Q. Li, $\Sigma_b \to \Sigma_c^*$ weak decays in the light-front quark model with two schemes to deal with the polarization of diquark, J. Phys. G **46**, 115003 (2019).
[161] W. Wang, F. S. Yu, and Z. X. Zhao, Weak decays of doubly heavy baryons: The $1/2 \to 1/2$ case, Eur. Phys. J. C **77**, 781 (2017).
[162] J. Zhu, Z. T. Wei, and H. W. Ke, Semileptonic and nonleptonic weak decays of Λ_b^0, Phys. Rev. D **99**, 054020 (2019).
[163] Z. X. Zhao, Weak decays of heavy baryons in the light-front approach, Chin. Phys. C **42**, 093101 (2018).
[164] Z. P. Xing and Z. X. Zhao, Weak decays of doubly heavy baryons: The FCNC processes, Phys. Rev. D **98**, 056002 (2018).
[165] C. K. Chua, Color-allowed bottom baryon to charmed baryon nonleptonic decays, Phys. Rev. D **99**, 014023 (2019).
[166] Z. X. Zhao, Weak decays of doubly heavy baryons: The $1/2 \to 3/2$ case, Eur. Phys. J. C **78**, 756 (2018).
[167] C. K. Chua, Color-allowed bottom baryon to s-wave and p-wave charmed baryon nonleptonic decays, Phys. Rev. D **100**, 034025 (2019).
[168] H. W. Ke, F. Lu, X. H. Liu, and X. Q. Li, Study on $\Xi_{cc} \to \Xi_c$ and $\Xi_{cc} \to \Xi_c'$ weak decays in the light-front quark model, Eur. Phys. J. C **80**, 140 (2020).
[169] H. W. Ke, N. Hao, and X. Q. Li, Revisiting $\Lambda_b \to \Lambda_c$ and $\Sigma_b \to \Sigma_c$ weak decays in the light-front quark model, Eur. Phys. J. C **79**, 540 (2019).
[170] X. H. Hu, R. H. Li, and Z. P. Xing, A comprehensive analysis of weak transition form factors for doubly heavy baryons in the light front approach, Eur. Phys. J. C **80**, 320 (2020).
[171] C. Q. Geng, C. C. Lih, C. W. Liu, and T. H. Tsai, Semileptonic decays of Λ_c^+ in dynamical approaches, Phys. Rev. D **101**, 094017 (2020).
[172] Y. K. Hsiao, L. Yang, C. C. Lih, and S. Y. Tsai, Charmed Ω_c weak decays into Ω in the light-front quark model, Eur. Phys. J. C **80**, 1066 (2020).
[173] Y. K. Hsiao and C. C. Lih, Fragmentation fraction f_{Ω_b} and the $\Omega_b \to \Omega J/\psi$ decay in the light-front formalism, Phys. Rev. D **105**, 056015 (2022).
[174] C. Q. Geng, C. W. Liu, and T. H. Tsai, Non-leptonic two-body decays of Λ_b^0 in light-front quark model, Phys. Lett. B **815**, 136125 (2021).
[175] H. W. Ke, Q. Q. Kang, X. H. Liu, and X. Q. Li, Weak decays of in the light-front quark model $*$, Chin. Phys. C **45**, 113103 (2021).
[176] Z. X. Zhao, Weak decays of triply heavy baryons: The $3/2 \to 1/2$ case, arXiv:2204.00759.
[177] C. Q. Geng, C. W. Liu, Z. Y. Wei, and J. Zhang, Weak radiative decays of antitriplet bottomed baryons in light-front quark model, Phys. Rev. D **105**, 073007 (2022).
[178] W. Wang and Z. P. Xing, Weak decays of triply heavy baryons in light front approach, Phys. Lett. B **834**, 137402 (2022).
[179] H. Liu, W. Wang, and Z. P. Xing, Baryonic heavy-to-light form factors induced by tensor current in light-front approach, Phys. Rev. D **108**, 035008 (2023).
[180] F. Lu, H. W. Ke, X. H. Liu, and Y. L. Shi, Study on the weak decay between two heavy baryons $\mathcal{B}_i(\frac{1}{2}^+) \to \mathcal{B}_f(\frac{3}{2}^+)$ in the light-front quark model, Eur. Phys. J. C **83**, 412 (2023).
[181] Z. X. Zhao, F. W. Zhang, X. H. Hu, and Y. J. Shi, Baryons in the light-front approach: The three-quark picture, Phys. Rev. D **107**, 116025 (2023).
[182] Y. S. Li, X. Liu, and F. S. Yu, Revisiting semileptonic decays of $\Lambda_{b(c)}$ supported by baryon spectroscopy, Phys. Rev. D **104**, 013005 (2021).
[183] Y. S. Li and X. Liu, Restudy of the color-allowed two-body nonleptonic decays of bottom baryons Ξ_b and Ω_b supported by hadron spectroscopy, Phys. Rev. D **105**, 013003 (2022).
[184] Y. S. Li, S. P. Jin, J. Gao, and X. Liu, Transition form factors and angular distributions of the $\Lambda_b \to \Lambda(1520)(\to N\bar{K})\ell^+\ell^-$ decay supported by baryon spectroscopy, Phys. Rev. D **107**, 093003 (2023).
[185] Y. S. Li and X. Liu, Investigating the transition form factors of $\Lambda_b \to \Lambda_c(2625)$ and $\Xi_b \to \Xi_c(2815)$ and the corresponding weak decays with support from baryon spectroscopy, Phys. Rev. D **107**, 033005 (2023).
[186] R. N. Faustov, V. O. Galkin, and X. W. Kang, Relativistic description of the semileptonic decays of bottom mesons, Phys. Rev. D **106**, 013004 (2022).
[187] G. Buchalla, A. J. Buras, and M. E. Lautenbacher, Weak decays beyond leading logarithms, Rev. Mod. Phys. **68**, 1125 (1996).
[188] R. L. Workman *et al.* (Particle Data Group), Review of particle physics, Prog. Theor. Exp. Phys. **2022**, 083C01 (2022).

[189] C. H. Chen and C. Q. Geng, Baryonic rare decays of $\Lambda_b \to \Lambda \ell^+ \ell^-$, Phys. Rev. D **64**, 074001 (2001).
[190] M. J. Aslam, Y. M. Wang, and C. D. Lü, Exclusive semileptonic decays of $\Lambda_b \to \Lambda \ell^+ \ell^-$ in supersymmetric theories, Phys. Rev. D **78**, 114032 (2008).
[191] G. M. Asatrian and A. Ioannisian, *CP* violation in the decay $b \to s\gamma$ in the left-right symmetric model, Phys. Rev. D **54**, 5642 (1996).
[192] A. J. Buras and M. Munz, Effective Hamiltonian for $B \to X_s e^+ e^-$ beyond leading logarithms in the NDR and HV schemes, Phys. Rev. D **52**, 186 (1995).
[193] A. Khodjamirian, T. Mannel, A. A. Pivovarov, and Y. M. Wang, Charm-loop effect in $B \to K^{(*)} \ell^+ \ell^-$ and $B \to K^* \gamma$, J. High Energy Phys. 09 (2010) 089.
[194] A. Khodjamirian, T. Mannel, and Y. M. Wang, $B \to K \ell^+ \ell^-$ decay at large hadronic recoil, J. High Energy Phys. 02 (2013) 010.
[195] Q. Qin, Y. L. Shen, C. Wang, and Y. M. Wang, Deciphering the long-distance penguin contribution to $\bar{B}_{d,s} \to \gamma\gamma$ decays, Phys. Rev. Lett. **131**, 091902 (2023).
[196] W. Altmannshofer, P. Ball, A. Bharucha, A. J. Buras, D. M. Straub, and M. Wick, Symmetries and asymmetries of $B \to K^* \mu^+ \mu^-$ decays in the standard model and beyond, J. High Energy Phys. 01 (2009) 019.
[197] J. Matias, F. Mescia, M. Ramon, and J. Virto, Complete anatomy of $\bar{B}_d \to \bar{K}^{*0}(\to K\pi) l^+ l^-$ and its angular distribution, J. High Energy Phys. 04 (2012) 104.
[198] S. Descotes-Genon, T. Hurth, J. Matias, and J. Virto, Optimizing the basis of $B \to K^* ll$ observables in the full kinematic range, J. High Energy Phys. 05 (2013) 137.
[199] A. K. Alok, N. R. Singh Chundawat, and A. Mandal, Investigating the potential of $R^{\tau\mu}_{K^{(*)}}$ to probe lepton flavor universality violation, arXiv:2303.16606.
[200] Y. Li and C. D. Lü, Recent anomalies in B physics, Sci. Bull. **63**, 267 (2018).
[201] M. Wirbel, B. Stech, and M. Bauer, Exclusive semileptonic decays of heavy mesons, Z. Phys. C **29**, 637 (1985).
[202] P. Ball and V. M. Braun, Exclusive semileptonic and rare B meson decays in QCD, Phys. Rev. D **58**, 094016 (1998).
[203] A. Ali, P. Ball, L. T. Handoko, and G. Hiller, A comparative study of the decays $B \to (K, K^{*)} \ell^+ \ell^-$ in Standard Model and supersymmetric theories, Phys. Rev. D **61**, 074024 (2000).
[204] X. J. Li, Y. S. Li, F. L. Wang, and X. Liu, Whole B_c meson spectroscopy under the unquenched picture, arXiv:2308.07206.
[205] R. Dhir and R. C. Verma, B_c meson form factors and $B_c \to PV$ decays involving flavor dependence of transverse quark momentum, Phys. Rev. D **79**, 034004 (2009).